Pinning Control of Networks: an Event-Triggered Approach

FRANCESCO ALDERISIO

KTH Electrical Engineering

Master's Degree Project

Stockholm, Sweden

November 2013

XR-EE-RT 2013:028

Master's Thesis

Pinning Control of Networks: an Event-Triggered Approach

Supervisors:
Prof. Dimos V. Dimarogonas
Dr. Davide Liuzza
Dr. Guodong Shi

Author:
Francesco Alderisio

Examiner:
Prof. Karl H. Johansson

Stockholm, Sweden
November 2013

Automatic Control
School of Electrical Engineering
KTH Royal Institute of Technology

Abstract

In this master thesis we present an algorithm for distributed event-triggered pinning control of a network of nonlinear oscillators.

In order to extend the concepts of connected, switching connected and slow switching topology to a pinning control scenario, we introduce the definitions of pinned, switching pinned and frequently pinned topology respectively.

For each of these three topologies we try to identify the conditions under which the network achieves exponential convergence of the error norm, find a lower bound for the rate of convergence and prove that the trigger sequences do not exhibit Zeno behavior.

Some numerical results are presented for each of the considered scenarios; further numerical results are presented for four elementary static topologies.

Contents

Chapter 1

Introduction

In this chapter we introduce the pinning control problem and we outline the difference between a pinning control problem and a synchronization problem.

In Section 1.1 we give a quick overview of the existing master thesis about synchronization and pinning control in a time-continuous fashion. Then we present the event-triggered approach in automatic control and we introduce its application to the problems of synchronization and pinning. We mention the self-triggered approach for completeness as well. In Section 1.2 we explain how our master thesis contributes to the ongoing research on event-triggered pinning control. In Section 1.3 we present some of the employed notations and properties. In Section 1.4 we review some well known concepts of elementary graph theory and then we introduce some new definitions specifically designed to address the pinning control problem. In Section 1.5 we define the mathematical model to which our analytical considerations and numerical experiments refer, giving a description of the plant that we would like to control in terms of the formalism introduced in Section 1.4. Then we provide a mathematical expression of the control law as well. Section 1.6 concludes the chapter with the outline of this master thesis.

1.1 Existing Work

The problem of synchronizing a multi-agent system has been widely addressed in the literature of the last decade. Among the countless real life applications of this problem, we can mention sensor fusion [1, 2], flocking [3], platooning and formation control [4, 5, 6] and synchronization of power grids [7]. An extensive list of applications in biology, neuroscience, computer science, engineering, social sciences and economy can be found in [8].

In its most basic formulation, this problem features a network of interacting first-order integrators and the aim is to drive them onto the average of their initial states applying an appropriate communication protocol. This is usually referred to as the *consensus problem*. When agents with more complicated dynamics are considered, the aim is to drive them onto a common trajectory, which in general is not known a priori. This is usually referred to as the *synchronization problem*.

In [9, 10] the consensus problem is addressed with linear and nonlinear interaction protocols, taking also into account possible time delays in the communication, while in [11, 12, 13] the problem of synchronizing networks of second-order integrators is addressed.

Of course a static interaction protocol among the agents is a too restrictive model for most real world applications. Communication failures, variations in the intensity of the interactions and formation of new communication channels must often be taken into account, leading to more complex yet realistic network models. Synchronization over time-varying topologies is addressed in [14, 15, 16] for integrators, in [17] for linear dynamical systems and in [18] for generic systems. Active variation of the interaction protocol is addressed in [19] for simple integrators, in [20] for linear dynamical systems, in [21] for nonlinear oscillators and in [22] for non identical nonlinear agents. Disconnected topologies have been recently addressed in [23] for simple integrators and in [24, 25] for generic systems.

A more challenging problem consists in driving a network of interacting agents onto a well defined reference trajectory. In this problem, usually referred to as *pinning control problem*, a feedback control law is applied to a small subset of the agents which are said to be *pinned*, while convergence of the other agents to the reference must be obtained thanks to their interactions with the pinned agents. Pinning control of nonlinear oscillators over a static topology is addressed in [26, 27]. Adaptation of interaction intensity is studied for pinning control of nonlinear oscillators in [28]. In [29] the concept of *pinning controllability* is defined in terms of the spectral properties of the network topology, and the roles of the coupling and control gains are discussed as well. In [30] criteria for global pinning controllability of networks of nonlinear oscillators are provided in terms of the network topology, the oscillator dynamics and the feedback control law. Strategies for optimal pin selection are presented in [31, 32]. In [33] analytical tools are developed to study the controllability of a network and to identify the optimal subset of driver nodes. Decentralized adaptive pinning strategies are introduced in [34, 35]. In [36] pinning control over a time-varying topology is investigated. Pinning control with nonlinear interaction protocol is studied in [37]. In [38] pinning controllability in networks with and without communication delay is investigated and a selective pinning criterion is proposed. In [39] local stochastic stability of networks under pinning control is studied, with stochastic perturbations to the interaction intensity. In [40] pinning control is applied to a network of non identical oscillators. Recently, an overview of the pinning control problem has been presented in [41].

In many real scenarios a large number of dynamical systems are supposed to communicate over a wireless medium, which represents a shared resource with limited capacity, and actuators might have a limited switching frequency. In addition to this, distributed control laws are supposed to be hosted and executed on small microprocessors embedded on the network agents. In such scenarios, time continuous interaction protocols and control laws become unrealistic assumptions, since they require uninterrupted information flow among the agents and continuous control updating. Limitations imposed by the network have been traditionally addressed via periodic updates. This approach creates both the problem of synchronization of sampling instants among the interconnected systems and the problem of simultaneous transmission of all the information over the network. Moreover, the sampling period must be chosen in order to guarantee stability and performance in all the possible operating conditions, thus leading to conservative results.

More recently, *event-triggered* control strategies have been introduced as an alternative to time-driven control updates. In such strategies, control updating and communication occur only when some conditions, usually related to the state of the network, are satisfied. On the other hand, if these conditions are not satisfied, the control signal is held constant and no communication takes place. Therefore with this mechanism the sampling rate is adapted according to the current condition of the network and unnecessary transmission of data is avoided. Particular attention is paid to avoiding the generation of an infinite number of events within a finite time interval.

Event-triggered designs have been developed for consensus algorithms and for control and synchronization of linear dynamical systems. Event-triggered control strategies are studied in [42, 43, 44, 45, 46, 47] for single dynamical systems. Event-triggered control is applied in [48] on a network of linear dynamical systems, while in [49, 50] on a network of simple integrators with particular attention on the comparison between a centralized and a decentralized approach. Event-triggered control for a network of non identical linear systems is addressed in [51]. In [52] event-triggered control is applied to integrators interacting over disconnected time-varying topologies. Event-based communication is applied to the consensus problem in [53] and in [54] taking into account possible communication delays and double integrators. On-line estimation of some topology characteristic is exploited in [55] to enhance the performances of event-triggered consensus algorithms. Performances obtainted with continuous, sampled and aperiodic updates over a nonlinear interaction protocol are compared in [56] for simple integrators. In [57] a model based event-triggered control algorithm is applied for synchronization of nonlinear oscillators.

In order to overcome the problem of checking continuously the triggering conditions, the *self-triggered* approach has been developed, in which every trigger instant is computed at the previous one using information on the state of the system currently available to the controller. Self-triggered control is applied for single nonlinear systems in [58]. In [59] self-triggered control is applied on a network of simple integrators with particular attention on the comparison between a centralized and a decentralized approach. A comprehensive introduction to both event-triggered and self-triggered control has been recently provided in [60].

1.2 Our Contribution

The main contribution of our master thesis is the application of a decentralized event-triggered approach on a pinning control scenario for a network of nonlinear systems. Our starting point is the novel algorithm presented in [57] for event-based synchronization of nonlinear oscillators. Besides, we apply pinning control to the oscillators in order to drive them onto a reference trajectory known a priori. Pinning controllability of the network is studied according to the criteria introduced in [30]. time-varying topologies are taken into account as well.

For each considered scenario we outline the hypotheses under which convergence to the reference trajectory can be achieved while avoiding accumulation points of events. Moreover, a lower bound for the rate of convergence is provided in each case.

1.3 Preliminary Notation and Properties

Let us now present some of the employed notations and properties.

The operator $| \ |$ on a set shall indicate the cardinality of that set. The operator $|| \ ||$ on a vector shall indicate the euclidean norm of that vector.

For a positive integer n we shall denote with 1_n the vector made up of n unitary components, and with I_n the identity matrix of order n.

The operator $\otimes$ between two matrices indicates the Kronecker product. Consider two square matrices $A \in \mathbb{R}_{N_a \times N_a}$ and $B \in \mathbb{R}_{N_b \times N_b}$. For $i = 1 \dots N_a$ we denote with a_i and α_i the i-th eigenvalue of matrix A and the corresponding eigenvector, while for $j = 1 \dots N_b$ we denote with b_j and β_j the j-th eigenvalue of matrix B and the corresponding eigenvector. Then the eigenvalues of matrix $A \otimes B$ are given by $\lambda_{ij} = a_i \; b_j$ while the corresponding eigenvectors are given by $v_{ij} = \alpha_i \otimes \beta_j$.

Consider four matrices A,B,C,D such that $A \cdot C$ and $B \cdot D$ are defined. Then it holds that $(A \otimes B) \cdot (C \otimes D) = (A \cdot C) \otimes (B \cdot D)$.

Given a vector $v \in \mathbb{R}_n$ we shall denote $v_{[N]} = 1_N \otimes v \in \mathbb{R}_{Nn}$.

A function $f : \mathbb{R}_n \to \mathbb{R}_n$ is said to be *one-side Lipschitz* with a *Lipschitz constant* L_f if for any $x, y \in \mathbb{R}_n$ it holds that $(x-y)^T[f(x)-f(y)] \leq L_f||x-y||^2$. It is said to be *globally Lipschitz* if $||f(x) - f(y)|| \leq L_f||x - y||$. It is easy to show that if a function is globally Lipschitz with a constant L_f, then it is also one-side Lipschitz with the same constant, while the reverse implication is not true.

A sequence of time instants $\mathcal{T} = \{t_k \in \mathbb{R}\}$ is said to exhibit *Zeno behavior* if there exists an interval $\mathcal{I} = [a, b] \subset \mathbb{R}$ such that for any $k > 0$ it holds that $|\mathcal{I} \cap \mathcal{T}| > k$. In other words, we say that a time sequence exhibits Zeno behavior if it has an accumulation point somewhere on the time axis.

Remark 1. *For a time sequence that exhibits Zeno behavior, there exists at least one finite time window in which infinite samples of said sequence can be found. Vice versa, absence of Zeno behavior guarantees that there is always a finite number of samples of that sequence in any finite time winodw, but this does not rule out the possibility of two consecutive samples being arbitrarily close to each other.*

1.4 Elements of Graph Theory

Let us consider a set $\mathcal{V} = \{1, 2, \ldots, N\}$ and a set $\mathcal{E} \subseteq \mathcal{V} \times \mathcal{V}$. The couple $\mathcal{G} = \{\mathcal{V}, \mathcal{E}\}$ is called a *graph*. The elements of $\mathcal{V}$ are called *nodes* of the graph while the elements of $\mathcal{E}$ are called *edges* of the graph.

If $(i, j) \in \mathcal{E} \iff (j, i) \in \mathcal{E}$ the graph is said to be *undirected*, otherwise it is said to be *directed*. If $(i, i) \notin \mathcal{E}\ \forall i \in \mathcal{V}$ the graph is said to be *simple*. All the graphs considered in our master thesis are simple and undirected. Therefore, all the definitions and properties given from now on are related to this particular kind of graphs.

In a simple undirected graph nodes i and j are said to be *neighbors* If $(i, j) \in \mathcal{E}$. The set of the neighbors of node i is denoted with $\mathcal{N}_i \subset \mathcal{V}$. The number $d_i = |\mathcal{N}_i|$ of the neighbors of node i is called *degree* of node i. The diagonal matrix $D = diag\{d_1, d_2, \ldots, d_N\}$ is called *degree matrix* of the graph. The maximum degree in the graph shall be denoted with Δ.

The matrix $A = A^T = \{a_{ij}\} \in \mathbb{R}_{N \times N}$ such that

$$a_{ij} = \begin{cases} 1 & \text{if nodes } i \text{ and } j \text{ are neighbors} \\ 0 & \text{otherwise} \end{cases} \tag{1.1}$$

is called *adjacency matrix* of the graph.

Thecan be shown that the Laplacian has zero row sum, and therefore it holds that $L \cdot 1_N = 0$. It is also easy to show that a Laplacian is positive semidefinite with at least one null eigenvalue.

A set $\mathcal{C} \subseteq \mathcal{V}$ is called a *component* of the graph if its nodes have no neighbors outside of $\mathcal{C}$ itself. When a component has no subset that is itself a component, it is said to be *connected*. It is possible to show that the number of null eigenvalues of the Laplacian coincides with the number of connected components in the graph.

The graph formalism provides an excellent starting point to model those control problems featuring a number of interacting systems. Nevertheless, by adding just a few more elements we can obtain a solid base to specifically tackle the pinning control problem.

Definition 1 (augmented graph). *Given a graph* $\mathcal{G} = \{\mathcal{V}, \mathcal{E}\}$*, let us consider a set* $\mathcal{P} \subseteq \mathcal{V}$*. The nodes belonging to* $\mathcal{P}$ *are said to be* pinned*. We shall denote with* r *the number of pinned nodes in the graph. Let us also consider two positive definite matrices* $\Gamma, K > 0$ *which we shall call* interaction protocol *and* control protocol *respectively. The norms of* Γ, K *shall be called* coupling *and* control strength *and shall be denoted with* γ, k *respectively. The set* $\tilde{\mathcal{G}} = \{\mathcal{V}, \mathcal{E}, \mathcal{P}, \Gamma, K\}$ *is called* augmented graph*. The diagonal matrix* $P = diag\{p_1, p_2 \dots p_N\}$ *such that*

$$p_i = \begin{cases} 1 & \textit{if node } i \textit{ is pinned} \\ 0 & \textit{otherwise} \end{cases} \tag{1.2}$$

is called pinning matrix *of the augmented graph. Finally, the matrix*

$$\tilde{L} = L \otimes \Gamma + P \otimes K \tag{1.3}$$

is called augmented Laplacian *of the augmented graph.*

It is immediate to see that the augmented Laplacian is a positive semidefinite matrix and that it has as many null eigenvalues as the number of connected components in the augmented graph that do not contain pin nodes. An augmented graph in which all the connected components contain at least one pin is said to be *pinned*. In Appendix A we prove that the augmented Laplacian of a pinned graph is positive definite.

The concept of augmented graph provides a formalism specifically designed to address the pinning control problem. It may be worth pointing out here that in general none of the elements of an augmented graph are necessarily supposed to be constant over time. According to the nature of the modeled problem, all the elements of an augmented graph may well be time-varying.

1.5 Problem Statement

Let us consider an augmented graph $\tilde{G} = \{\mathcal{V}, \mathcal{E}, \mathcal{P}, \Gamma, K\}$. For the moment being, let us assume that the graph is fixed, meaning that all its elements are constant over time.

To each node of the graph, let us associate a nonlinear system whose state is denoted with $x_i \in \mathbb{R}_n$ and whose dynamics is described by

$$\dot{x}_i = f(x_i) + u_i \tag{1.4}$$

Let function f be globally Lipschitz with a Lipschitz constant L_f. Let us assume that we want all the systems to synchronize onto an a-priori known reference trajectory $s(t)$, whose evolution is described by $\dot{s} = f(s)$. We shall call this goal *complete synchronization.* It is easy to see that complete synchronization may be formalized as

$$\lim_{t \to +\infty} ||s - x_i|| = 0 \qquad i = 1 \dots N \tag{1.5}$$

For $i, j = 1 \dots N$, let us introduce the mismatches $e_i = s - x_i$ and $e_{ij} = x_j - x_i = e_i - e_j$.

For each node i, let us define a sequence of time instants $\{t_k^i\}$ and let us assume that the control input u_i is calculated as

$$u_i = c \sum_{j=1}^{N} a_{ij} \Gamma e_{ij}(t_k^i) + c p_i K e_i(t_k^i) \qquad t \in [t_k^i, t_{k+1}^i) \tag{1.6}$$

where $A = A^T = \{a_{ij}\}$ and $P = diag\{p_1 \dots p_N\}$ are the adjacency and the pinning matrix of $\tilde{\mathcal{G}}$ respectively and c is the *control gain.* The control gain can be time-varying, but it is bounded by $0 < c \leq c_M$. Instants t_k^i are also called *events* or *triggers* for node i.

Our problem is to outline a set of hypotheses under which the described network achieves complete synchronization with absence of Zeno behavior for all the time sequences $\{t_k^i\}$.

Remark 2. *Note that the control signal does not vary in a time-continuous fashion, but it is held constant within each of the intervals* $[t^i_k, t^i_{k+1})$*. When a new sample of the time sequence* t^i_k *occurs, signal* u_i *is updated.*

1.6 Outline

The remainder of this master thesis is organized as follows. In Chapter 2 we propose a distributed algorithm for the generation of the trigger sequences designed to work on static topologies. Then we show that, under opportune hypotheses, this algorithm leads to complete synchronization with absence of Zeno behavior. In Chapters 3 and 4 we modify the given control algorithm in order to extend the results found for static topologies to switching pinned and frequently pinned topologies respectively. Throughout these chapters, theoretical results are confirmed by numerical simulations. Chapter 5 presents further numerical simulations on some static fundamental topologies. Chapter 6 concludes the master thesis with a summary of the main results and some suggestions for future developments.

Chapter 2

Static Topologies

In this chapter we consider networks whose topology does not vary over time, meaning that all the elements that define the augmented graph are fixed, and we aim at individuating the hypotheses under which complete synchronization can be achieved with absence of Zeno behavior.

In Section 2.1 we describe in detail the control algorithm employed to reach our goal. In Section 2.2 we prove that, under opportune hypotheses, the described control algorithm indeed achieves the goal of complete synchronization. In Section 2.3 we reflect on how these hypotheses can be fulfilled by acting on the parameters of the network. In Section 2.4 we prove that, under slightly more restrictive hypotheses, the time sequences defined in our algorithm do not exhibit Zeno behavior. Finally in Section 2.5 we describe the network that we have considered for numerical validation of our algorithm.

2.1 Algorithm Definition

Let us introduce the following *state measurement errors*, $\tilde{e}_i(t) = e_i(t_k^i) - e_i(t)$ and $\tilde{e}_{ij} = e_{ij}(t_k^i) - e_{ij}(t)$. Let us consider a *threshold function* $\varsigma(t) = k_\varsigma e^{-\lambda_\varsigma t}$ with $k_\varsigma, \lambda_\varsigma > 0$. For each node i of the graph, we update the time sequence $\{t_k^i\}$ according to the following rule.

Update Rule 1. *Instant* t^i_{k+1} *is the earliest instant* t *after* t^i_k *when one of the following conditions is satisfied:*

- $||\tilde{e}_{ij}(t)|| \geq \varsigma(t)$ *for some neighbor* j *of node* i*;*
- $||\tilde{e}_i(t)|| \geq \varsigma(t)$ *and node* i *is pinned.*

It is easy to see that if we apply Update Rule 1, at any time t the following conditions will hold.

$$\begin{cases} ||\tilde{e}_{ij}(t)|| < \varsigma(t) & \text{for all couples } (i,j) \text{ of neighbors} \\ ||\tilde{e}_i(t)|| < \varsigma(t) & \text{for all pinned nodes } i \end{cases} \tag{2.1}$$

Remark 3. *We notice that, even if errors* e_i *are defined for all nodes, in order to implement the control signals* u_i *we need to evaluate only those associated to pin nodes. No information about the state of nodes that are not pinned is considered when computing* u_i*. Similiarly, even if errors* e_{ij} *are defined for all couples* (i,j)*, the control signal* u_i *takes into account only the mismatches relative to neighbors of node* i*. No information is needed to be exchanged between nodes that are not neighbors.*

Thanks to Update Rule 1 it is now possible to give a detailed outline of the control algorithm adopted for the network.

- *Step 1.* Each of the agents is initialized at a state x_{i0}. The reference trajectory is also initialized at a state s_0. All the time sequences $\{t^i_k\}$ are initialized with $t^i_0 = 0$.
- *Step 2.* The control signals are computed according to equation (1.6). The agents states evolve according to (1.4). The reference trajectory also evolves according to its dynamics. For each node i, Update Rule 1 is employed. If node i satisfies the requirements of this rule, sequence $\{t^i_k\}$ is updated and the state measurement errors related to such node are reset.
- *Step 3.* Repeat from Step 2.

Remark 4. *It is worth pointing out here that in order to check condition* (2.1) *for itself, an agent needs to know not only its own state but also the state of all its neighbors at every time instant. This can be accomplished in two ways. The first way consists in neighboring agents communicating their state to each other continuously. The second way consists in each agent broadcasting its own control input to its neighbors any time it is updated to a new value. This allows an agent to predict the evolution of its neighbors' state.*

Note that the first method requires a larger information flow across the network, while the second one requires a higher computational capacity from the single agents. Which method is more convenient depends tightly on the considered application.

2.2 Complete Synchronization

In this section we prove that, under opportune hypotheses, the described control algorithm achieves the goal of complete synchronization. We also give a lower bound for the convergence rate of the error norm.

Hypothesis 1. *Function f is one-side Lipschitz with Lipschitz constant L_f and the minimum eigenvalue λ of the augmented Laplacian of the network satisfies $c\lambda > L_f$.*

Theorem 1. *Under Hypothesis 1, network* (1.4) *with control signal* (1.6) *and Update Rule 1 achieves complete synchronization as defined in* (1.5)*. Moreover, convergence to zero of the error norm is exponential with rate $\lambda_c = \min\{c\lambda - L_f, \lambda_\varsigma\} > 0$.*

Proof. We divide the proof in two parts. In the first part we find an upper bound for the time-derivative of the error norm. In the second part we integrate the expression of this bound and we apply the comparison lemma to upper-bound the error norm with a negative exponential. □

2.2.1 Upper Bound for the Time-Derivative of the Error Norm

For each node i, let us consider the dynamics of the mismatch.

$$\dot{e_i} = \dot{s} - \dot{x_i} = f(s) - f(x_i) - u_i \tag{2.2}$$

Upon substitution of u_i with its expression we get

$$\dot{e_i} = f(s) - f(x_i) - c\sum_{j=1}^{N} a_{ij}\Gamma e_{ij}(t_k^i) - cp_i K e_i(t_k^i) \tag{2.3}$$

Now let us introduce the error stack $e = [e_1^T e_2^T \dots e_N^T]^T$. It is easy to see that complete synchronization as defined in (1.5) corresponds to convergence to zero of the norm of e. Now let us observe that

$$\frac{1}{2}\frac{d}{dt}||e||^2 = \frac{1}{2}\frac{d}{dt}e^T e = e^T\dot{e} = \sum_{i=1}^{N} e_i^T \dot{e}_i \tag{2.4}$$

Substituing $\dot{e}_i$ with expression (2.2) we get

$$\frac{1}{2}\frac{d}{dt}||e||^2 = \sum_{i=1}^{N} e_i^T \left[f(s) - f(x_i) - c\sum_{j=1}^{N} a_{ij}\Gamma e_{ij}(t_k^i) - cp_i K e_i(t_k^i)\right] \tag{2.5}$$

Now let us substitute $\tilde{e}_i = e_i(t_k^i) - e_i$ and $\tilde{e}_{ij} = e_{ij}(t_k^i) - e_{ij}$ into the previous expression, obtaining

$$\begin{aligned}\frac{1}{2}\frac{d}{dt}||e||^2 = &\sum_{i=1}^{N} e_i^T[f(s) - f(x_i)] - c\sum_{i=1}^{N} p_i e_i^T K e_i - c\sum_{i=1}^{N} p_i e_i^T K \tilde{e}_i \\ &- c\sum_{i=1}^{N} e_i^T \sum_{j=1}^{N} a_{ij}\Gamma e_{ij} - c\sum_{i=1}^{N} e_i^T \sum_{j=1}^{N} a_{ij}\Gamma \tilde{e}_{ij}\end{aligned} \tag{2.6}$$

Now we would like to find an upper bound for this derivative. To this aim, we will bound each of the five addends separately.

Thanks to the one-side Lipschitzianity of function f, the first addend is upper-bounded by

$$\sum_{i=1}^{N} e_i^T [f(s) - f(x_i)] \leq L_f e^T e \tag{2.7}$$

Using triangular inequality and condition (2.1), we can bound the third and the fifth addend respectively with

$$c \sum_{i=1}^{N} p_i e_i^T K \tilde{e}_i \leq ck\varsigma \sum_{i=1}^{N} p_i ||e_i|| \leq c_M kr\varsigma ||e|| \tag{2.8}$$

$$c \sum_{i=1}^{N} e_i^T \sum_{j=1}^{N} a_{ij} \Gamma \tilde{e}_{ij} \leq c\gamma\varsigma \sum_{i=1}^{N} d_i ||e_i|| \leq c_M \gamma \Delta \sqrt{N} \varsigma ||e|| \tag{2.9}$$

The second and the fourth addend can be easily rewritten using the Kronecker product, yielding respectively

$$c \sum_{i=1}^{N} e_i^T \sum_{j=1}^{N} a_{ij} \Gamma e_{ij} = ce^T (L \otimes \Gamma) e \tag{2.10}$$

$$c \sum_{i=1}^{N} p_i e_i^T K e_i = ce^T (P \otimes K) e \tag{2.11}$$

Since the augmented Laplacian is positive semidefinite, we can sum these two addends and easily bound them together with

$$ce^T (L \otimes \Gamma + P \otimes K) e \geq c\lambda ||e||^2 \tag{2.12}$$

So, if we define for convenience $\beta = c_M (kr + \gamma \Delta \sqrt{N}) > 0$, we can finally bound equation (2.6) with

$$\frac{1}{2} \frac{d}{dt} ||e||^2 \leq L_f ||e||^2 + \beta\varsigma ||e|| - c\lambda ||e||^2 \tag{2.13}$$

Now let us observe that

$$\frac{1}{2} \frac{d}{dt} ||e||^2 = ||e|| \ \frac{d}{dt} ||e|| \tag{2.14}$$

Therefore we can rewrite (2.13) as

$$\frac{d}{dt}||e|| \leq (L_f - c\lambda)||e|| + \beta\varsigma \tag{2.15}$$

which concludes the first part of the proof.

Remark 5. *Note that in the last passage we have divided both members of the inequality by $||e||$, assuming implicitly that $||e|| > 0$. In the event of $||e|| = 0$ there are two possibilities. If the control inputs are also null, then the error stays in zero permanently, which means that complete synchronization has been achieved. If the control inputs are non null, then the time interval in which $||e|| = 0$ has null Lebesgue measure, which makes it inifluential when the inequality is integrated.*

2.2.2 Upper Bound for the Error Norm

For the sake of convenience let us define $\eta = ||e||$ so that we can rewrite (2.15) as

$$\dot{\eta}(t) \leq (L_f - c\lambda)\eta(t) + \beta\varsigma(t) \qquad \forall t \geq 0 \tag{2.16}$$

Let us integrate inequality (2.16) on an interval $[0, t]$ via Laplace's formula. Thanks to the comparison lemma [61], we obtain

$$\eta(t) \leq e^{(L_f - c\lambda)t}\eta_0 + \beta \int_0^t e^{(L_f - c\lambda)(t-\tau)}\varsigma(\tau)\ d\tau \qquad \forall t \geq 0 \tag{2.17}$$

where we have denoted $\eta_0 = \eta(0)$. If we substitute $\varsigma(\tau)$ with its expression we obtain

$$\eta(t) \leq e^{(L_f - c\lambda)t}\eta_0 + \beta k_\varsigma e^{(L_f - c\lambda)t} \int_0^t e^{-(\lambda_\varsigma + L_f - c\lambda)\tau}\ d\tau \tag{2.18}$$

Now, noting that

$$\int_0^t e^{-(\lambda_\varsigma + L_f - c\lambda)\tau}\ d\tau = \frac{1 - e^{-(\lambda_\varsigma + L_f - c\lambda)t}}{\lambda_\varsigma + L_f - c\lambda} \tag{2.19}$$

we can rewrite (2.18) as

$$\eta(t) \leq e^{(L_f - c\lambda)t}\eta_0 + \beta k_\varsigma \frac{e^{(L_f - c\lambda)t} - e^{-\lambda_\varsigma t}}{\lambda_\varsigma + L_f - c\lambda} \tag{2.20}$$

Therefore, if we define $\lambda_c = \min\{c\lambda - L_f, \lambda_\varsigma\}$, it holds that

$$\eta(t) \leq \left(\eta_0 + \frac{\beta k_\varsigma}{|\lambda_\varsigma + L_f - c\lambda|}\right) e^{-\lambda_c t} \tag{2.21}$$

Thanks to Hypothesis 1 and to the definition of ς as a decreasing exponential with rate of convergence $\lambda_\varsigma > 0$, we can easily state that $\lambda_c > 0$, thus concluding the proof of complete synchronization.

Remark 6. *We have not considered explicitly the case of $\lambda_\varsigma + L_f - c\lambda = 0$, in which integration* (2.19) *is not true, and the integral yields t instead. However, in this case we have $\lambda_\varsigma = c\lambda - L_f$, so that we can rewrite* (2.18) *as*

$$\eta(t) \leq (\eta_0 + \beta k_\varsigma t)\, e^{-\lambda_\varsigma t} \tag{2.22}$$

Since t can be upper-bounded with any positive exponential, we still achieve convergence with an exponential rate as close to λ_ς as desired. Specifically, for any $\epsilon > 0$ we can write $t < \frac{e^{\epsilon t}}{\epsilon}$, so that we have

$$\eta(t) \leq \left(\eta_0 + \frac{\beta k_\varsigma}{\epsilon}\right) e^{-(\lambda_\varsigma - \epsilon)t} \tag{2.23}$$

2.3 Topology Requirements for Complete Synchronization

Now that we know that a condition for convergence is that $c\lambda > L_f$, let us reflect on how this requirement can be fulfilled by acting on the parameters of the network.

First of all we need that $\lambda > 0$. We have mentioned in Section 1.4 that the augmented Laplacian is positive definite if the augmented graph is pinned, meaning that all the connected components must contain at least one pin node. Therefore, in order to get $\lambda > 0$ we must make sure that all the connected components of the graph contain at least one pin node. This makes perfect sense since, if a connected component did not contain any pin, then its nodes would not be influenced at all by the reference trajectory. Proof of this property can be deduced from results available in graph theory about more general kinds of graphs. Nevertheless, in Appendix A we propose a version of such proof specifically designed to address the augmented graph formalism.

Assuming that the graph is pinned, the minimum eigenvalue of the augmented Laplacian can be largely influenced by variations in the topology of the connections and in the location of the pin nodes. Given a fixed number of edges and pins, their optimal disposition among the nodes is, in general, a highly non trivial problem. For a given topology of connections some criteria for optimal pin selection may be derived algebrically. We address this problem for a limited number of fundamental topologies in our second master thesis. Note that even if the interconnections and the location of the pins are given, λ is still influenced by the norms and the structure of the communication and control protocols.

Of course, even if we assume that the augmented graph for the network is assigned, so that λ cannot be changed, Hypothesis 1 can be satisfied selecting an appropriate value of the control gain c. Indeed, if λ is known it is always possible to pick a gain which is large enough to satisfy the hypothesis.

Remark 7. *We have pointed out that, theorically, it is always possible to select a control gain c which is large enough to satisfy Hypothesis 1. Obviously in real applications some constraints have to be put on the gain in order to limit the energy employed in the process. However, analytical reasons can also be found to limit the value assumed by c. For example, since β is proportional to c_M, a smaller upper bound on the control gain results in a better upper bound for the trajectory of the error norm.*

2.4 Absence of Zeno Behavior

In this section we prove that, under opportune hypotheses, the time sequences defined in our algorithm do not exhibit Zeno behavior.

Hypothesis 2. *Function f is globally Lipschitz with Lipschitz constant L_f and the minimum eigenvalue λ of the augmented Laplacian of the network satisfies $c\lambda > L_f + \lambda_\varsigma$.*

Theorem 2. *Under Hypothesis 2 the time sequences $\{t_k^i\}$ with $i = 1 \dots N$ do not exhibit Zeno behavior.*

Proof. The proof of this theorem is divided in two parts. In the first part we find upper bounds for the norm of the time-derivative of all the mismatches, while in the second part we use such bounds to show that two consecutive samples belonging to the same sequence are separated by a strictly positive inter-event time. □

2.4.1 Upper Bounds for the Time-Derivative of the Mismatches

First of all let us observe that under Hypothesis 2, inequality (2.21) holds, and in particular it can be rewritten as

$$\eta \leq \left(\eta_0 + \frac{\beta k_\varsigma}{c\lambda - \lambda_\varsigma - L_f} \right) e^{-\lambda_\varsigma t} = \chi \varsigma \tag{2.24}$$

where we have defined

$$\chi = \frac{\eta_0}{k_\varsigma} + \frac{\beta}{c\lambda - \lambda_\varsigma - L_f} > 0 \tag{2.25}$$

Let us now consider the dynamics of the mismatch e_i for each node i.

$$\dot{e}_i = f(s) - f(x_i) - c \sum_{j=1}^{N} a_{ij} \Gamma(e_{ij} + \tilde{e}_{ij}) - c p_i K(e_i + \tilde{e}_i) \tag{2.26}$$

Application of the triangular inequality yields

$$||\dot{e}_i|| \leq ||f(s) - f(x_i)|| + c\gamma \sum_{j=1}^{N} a_{ij}(||e_{ij}|| + ||\tilde{e}_{ij}||) + ckp_i(||e_i|| + ||\tilde{e}_i||) \quad (2.27)$$

Now we are going to upper-bound each of the addends separately. Thanks to global Lipschitzianity of function f, and noting that $||e_i|| \leq \eta \leq \chi\varsigma$, we can bound the first addend with

$$||f(s) - f(x_i)|| \leq L_f||e_i|| \leq L_f\chi\ \varsigma \quad (2.28)$$

Thanks to condition (2.1), and noting that $||e_{ij}|| \leq ||e_i|| + ||e_j|| \leq 2\eta$, the second addend can be upper-bounded by

$$c\gamma \sum_{j=1}^{N} a_{ij}(||e_{ij}|| + ||\tilde{e}_{ij}||) \leq c_M\gamma(2\chi + 1)d_i\ \varsigma \quad (2.29)$$

while the third addend can be upper-bounded by

$$ckp_i(||e_i|| + ||\tilde{e}_i||) \leq c_M kp_i(\chi + 1)\ \varsigma \quad (2.30)$$

Therefore we can finally bound $||\dot{e}_i||$ with

$$||\dot{e}_i|| \leq [L_f\chi + c_M\gamma(2\chi + 1)d_i + c_M kp_i(\chi + 1)]\varsigma = \omega_i\varsigma \quad (2.31)$$

where we have defined

$$\omega_i = L_f\chi + c_M\gamma(2\chi + 1)d_i + c_M kp_i(\chi + 1) > 0 \quad (2.32)$$

Let us now consider the dynamics of the mismatches $\dot{e}_{iq}$ for each couple of nodes i, q in the network. Since $\dot{e}_{iq} = \dot{e}_i - \dot{e}_q$, we can apply triangular inequality and obtain $||\dot{e}_{iq}|| \leq ||\dot{e}_i|| + ||\dot{e}_q||$, which thanks to (2.31) becomes

$$||\dot{e}_{iq}|| \leq (\omega_i + \omega_q)\varsigma \quad (2.33)$$

which concludes the first part of the proof.

2.4.2 Lower Bound for the Inter-Event Time

We are now going to bound the norms of the state measurement errors. First let us observe that for $t_k^i \leq t < t_{k+1}^i$ it holds that

$$||\tilde{e}_i(t)|| = \left|\left|\int_{t_k^i}^{t} -\dot{e}_i(\tau)\ d\tau\right|\right| \leq \int_{t_k^i}^{t} ||\dot{e}_i(\tau)||\ d\tau \leq \omega_i \int_{t_k^i}^{t} \varsigma(\tau)\ d\tau \tag{2.34}$$

Now since ς is a nonincreasing function, the inequality can be rewritten as

$$||\tilde{e}_i(t)|| \leq \omega_i \varsigma(t_k^i)(t - t_k^i) \tag{2.35}$$

This means that in order for condition $||\tilde{e}_i|| < \varsigma$ to be violated after instant t_k^i, it is necessary to wait at least until an instant $t \geq t_k^i$ which satisfies

$$\omega_i \varsigma(t_k^i)(t - t_k^i) = \varsigma(t) \tag{2.36}$$

Substituting ς with its expression we obtain

$$\omega_i(t - t_k^i) = e^{-\lambda_\varsigma(t - t_k^i)} \tag{2.37}$$

whose solution in terms of $t - t_k^i$ is strictly positive. Reasoning in the very same way for $||\tilde{e}_{iq}||$, the following inequality holds

$$||\tilde{e}_{iq}(t)|| \leq (\omega_i + \omega_q)\varsigma(t_k^i)(t - t_k^i) \tag{2.38}$$

This means that in order to violate condition $||\tilde{e}_{iq}|| < \varsigma$ after instant t_k^i, it is necessary to wait at least until an instant $t \geq t_k^i$ which satisfies

$$(\omega_i + \omega_q)(t - t_k^i) = e^{-\lambda_\varsigma(t - t_k^i)} \tag{2.39}$$

This time the solution in terms of $t - t_k^i$ is lower than in the previous case, but still it is strictly positive. Therefore we can state that the inter-event time between two consecutive samples of the sequence $\{t_k^i\}$ is lower-bounded by

$$\min_{j \in \mathcal{N}_q} \{\tau > 0 : (\omega_i + \omega_q)\tau = e^{-\lambda_\varsigma \tau}\} \tag{2.40}$$

This implies that Zeno behavior is excluded.

Remark 8. *Note that in this case we have proved that sequences $\{t_k^i\}$ have finite inter-event times, which is a stronger property than absence of Zeno behavior. In the following sections, when we try to extend our results to graphs with time-varying topologies, we will not be able to retain finiteness of the inter-event times.*

2.5 Numerical Experiments

In this section we are going to describe the network we have considered for numerical validation of our algorithm on a pinned topology scenario. Moreover, we show that complete synchronization can be achieved with absence of Zeno behavior thanks to an appropriate choice of the control parameters.

In our experiments the network is made up of N identical Chua's oscillators whose dynamics is described by the following equation

$$\begin{cases} \dot{x}_1 = a(x_2 - x_1 - \phi(x_1)) \\ \dot{x}_2 = x_1 - x_2 + x_3 \\ \dot{x}_3 = -bx_2 \end{cases} \tag{2.41}$$

where

$$\phi(y) = m_1 y + \frac{1}{2}(m_0 - m_1)(|y+1| - |y-1|) \qquad y \in \mathbb{R} \tag{2.42}$$

For parameters a, b, m_0 and m_1 we have chosen the following values:

$$a = 1 \quad b = 1 \quad m_0 = -1.5 \quad m_1 = -0.5 \tag{2.43}$$

With this choice it is possible to see that function f is globally Lipschitz with constant $L_f \simeq 3.75$. We do not know whether this choice is realistic, but it allows us to have a small value for the Lipschitz constant L_f. This means that in order to satisfy Hypothesis 2 we can choose a small value for the control gain c, thus allowing the simulation to run more smoothly.

The network is made up of $N = 10$ nodes and $r = 2$ of them are pinned. The network topology has been generated by selecting randomly $N_e = 24$ edges among all the possible ones.

As interaction protocol and control protocol we choose $\Gamma = I_n$ and $K = 4\, I_n$, respectively. The pinning matrix P is built by selecting the r pins which maximize the minimum eigenvalue of the augmented Laplacian. As for the parameters of the threshold function we choose $k_\varsigma = 0.1$ and $\lambda_\varsigma = 0.5$, so that Hypothesis 2 is satisfied with a constant control gain worth $c = \phi\, \frac{L_f + \lambda_\varsigma}{\lambda} \simeq 10.7$ where we choose $\phi = 1.2$. Finally, we choose initial conditions randomly.

Figures 2.1 and 2.2 show the trend of x_1 and e_1 during the simulation.

In Figures 2.3, 2.4 and 2.5 we show some variables of interest with regard to the frequency of trigger events.

Figure 2.1: trend of the first state variable for nodes $i = 1 \ldots 10$ - static topology scenario

(a) state

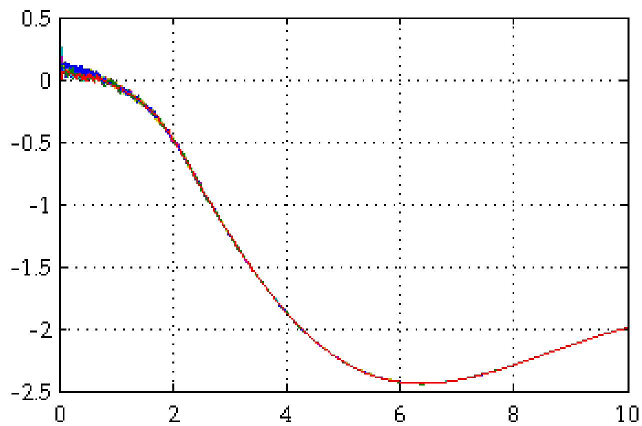

(b) state - zoom

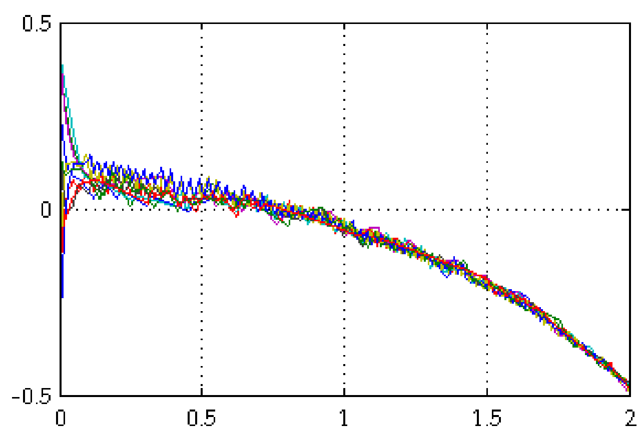

Figure 2.2: trend of the first error variable for nodes $i = 1 \ldots 10$ - static topology scenario

(a) error

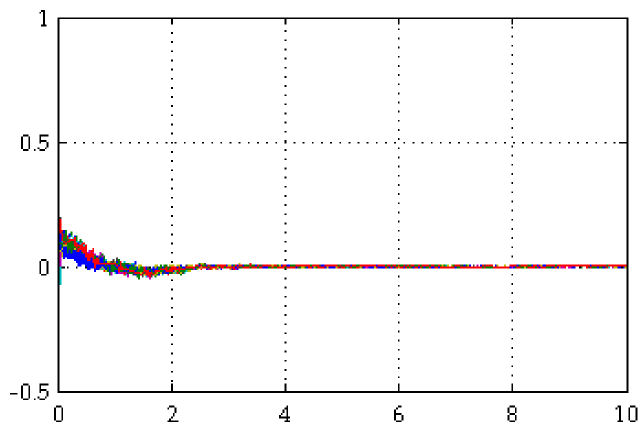

(b) error - zoom

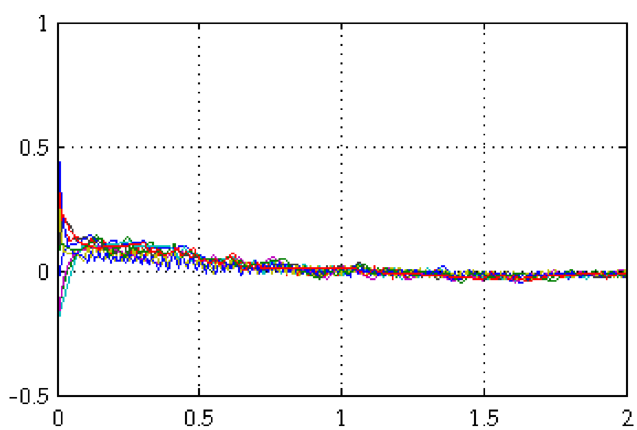

Figure 2.3: trigger events for nodes $i = 1 \dots 10$ - static topology scenario

(a) first second of the simulation

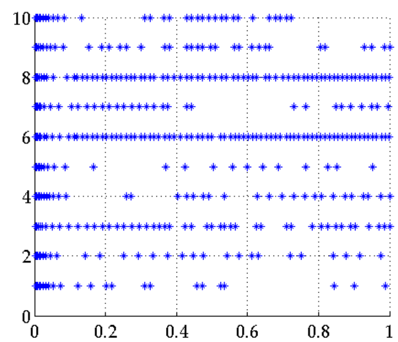

(b) last second of the simulation

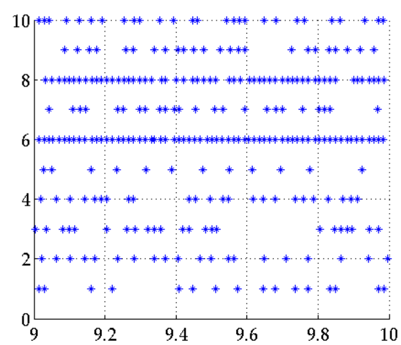

Figure 2.4: inter-event time lower bounds for nodes $i = 1 \dots 10$ - static topology scenario

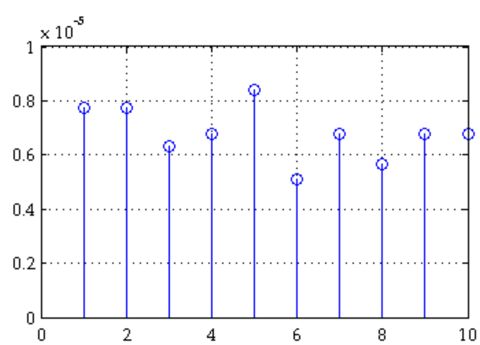

Figure 2.5: trend of the first control variable for nodes $i = 1 \dots 10$ - static topology scenario

(a) control

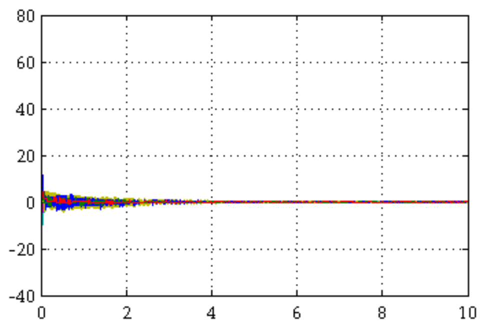

(b) control - zoom - first second of the simulation

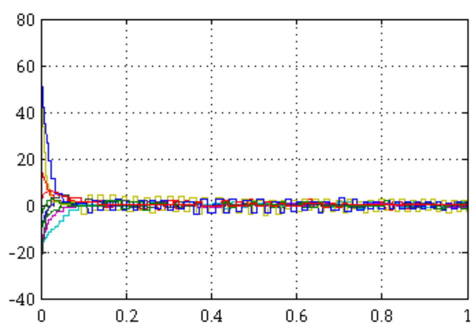

(c) control - zoom - last second of the simulation

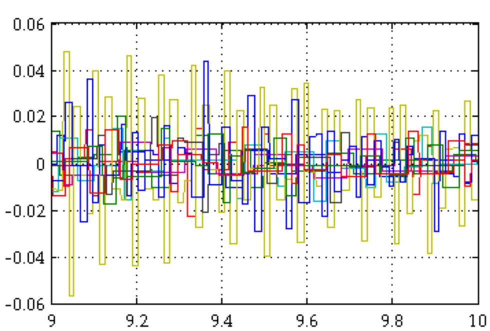

Chapter 3

Switching Pinned Topologies

In this chapter we consider a particular class of networks with time-varying topologies and parameters, and we aim at individuating the hypotheses under which the results found for static topologies still hold.

In Section 3.1 we give a detailed description of this particular class of networks. In Section 3.2 we describe the control algorithm employed to reach our goal. In Section 3.3 we prove that, under opportune hypotheses, the described control algorithm achieves the goal of complete synchronization. In Section 3.4 we reflect on how these hypotheses can be fulfilled by acting on the parameters of the network. In Section 3.5 we prove that, under slightly more restrictive hypotheses, the time sequences defined in our algorithm do not exhibit Zeno behavior. Finally in Section 3.6 we describe the network that we have considered for numerical validation of our algorithm.

3.1 Definition of Switching Pinned Topologies

In the scenario we would like to address, new connections may be generated, existing connections may be cut off, new pins may be introduced and existing pins may be removed. This means that L and P are two time-varying matrices. Such changes occur at discrete time instants, with non infinite frequency, but not necessarily at regular intervals. Conversely, the intensity of the control gain c may be varied in a time-continuous fashion.

In order to address the described scenario, let us introduce a special class of time-varying augmented graph, which we shall call *switching*.

Definition 2 (switching graph)**.** *A time-varying augmented graph is said to be* switching *with a* dwell time $\tau_d > 0$ *if*

- *the node set is constant;*

- *the edge set and the pin set may be modified at discrete time instants, but the degree of a node and the number of pin nodes are upper-bounded by some strictly positive constants* Δ_M *and* r_M*; morevoer, two consecutive variations are separated by a time interval at least worth* τ_d*;*

- *the interaction protocol* Γ *and control protocol* K*, and as a conseqence the coupling strength* γ *and the control strength* k*, are constant.*

Variations in the edge set and the pin set are called switchings*.*

Thanks to the previous definition, it is possible to introduce now a more restrictive class of time-varying augmented graph, which we shall call *switching pinned.*

Definition 3 (switching pinned graph)**.** *A switching graph is said to be* pinned *if it is pinned for any time* $t \geq 0$*.*

3.2 Algorithm Description

In order to design a version of our algorithm that can work on switching graphs, let us make the following observations.

When a switching causes a node i that was not pinned to become a pin node, error $e_i(t_k^i)$ is needed in order to calculate the control signal u_i. But e_i was not being measured, since node i was not a pin node. Therefore we believe that it is necessary to generate a trigger event for sequence $\{t_k^i\}$ whenever a switching that causes node i to become a pin node occurs.

Similiarly, when a switching causes a pair (i, j) to become neighbors, error $e_{ij}(t_k^i)$ is needed in order to calculate the control signal u_i. But since nodes i and j were not neighbors, the mismatch e_{ij} was not being monitored. Therefore we believe that it is necessary to generate a trigger event for sequence $\{t_k^i\}$ whenever a switching that causes node i to acquire a new neighbor occurs.

Hence we update sequence $\{t_k^i\}$ according to the following rule.

Update Rule 2. *Instant t_{k+1}^i is the earliest instant t after t_k^i when one of the following conditions is satisfied:*

- $||\tilde{e}_{ij}|| \geq \varsigma$ *for some neighbor j of node i;*
- *node i acquires a new neighbor because of a switching, that is* $a_{ij} - a_{ij}(t_k^i) = 1 \quad \textit{for some} \quad j = 1 \ldots N$
- $||\tilde{e}_i|| \geq \varsigma$ *and node i is pinned;*
- *node i becomes a pin node because of a switching, that is* $p_i - p_i(t_k^i) = 1$.

Therefore condition (2.1) still holds for all $t \geq 0$.

The control algorithm is the same as the one described for a static topology, with the only difference that Update Rule 2 is used instead of Update Rule 1 in *Step 2*.

3.3 Complete Synchronization

In this section we prove that, under opportune hypotheses, the described control algorithm achieves the goal of complete synchronization. We also give a lower bound for the convergence rate of the error norm.

In particular we extend the proof of complete synchronization to the case of switching graphs. We use the very same passages as in the static case, but the upper bounds that we introduce are slightly more conservative in order to deal with the time-dependence of the parameters.

Hypothesis 3. *Function f is one-side Lipschitz with Lipschitz constant L_f and there exists a constant $\psi > 0$ such that the minimum eigenvalue λ of the augmented Laplacian of the network satisfies $c\lambda - L_f \geq \psi$ for all $t \geq 0$.*

Theorem 3. *Under Hypothesis 3, network* (1.4) *with control signal* (1.6) *and Update Rule 2 achieves complete synchronization as defined in* (1.5)*. Morevoer, convergence to zero of the error norm is exponential with rate $\lambda_c = \min\{\psi, \lambda_\varsigma\} > 0$.*

Proof. We start as in Subsection 2.2.1, but since the number of pin nodes and the degrees of the nodes are time-varying, we adopt a worst-case approach and instead of inequalities (2.8), (2.9) we use the following bounds.

$$c\sum_{i=1}^{N} p_i e_i^T K\tilde{e}_i \leq ck\varsigma\sum_{i=1}^{N} p_i||e_i|| \leq c_M k r_M \varsigma||e|| \tag{3.1}$$

$$c\sum_{i=1}^{N} e_i^T \sum_{j=1}^{N} a_{ij}\Gamma\tilde{e}_{ij} \leq c\gamma\varsigma\sum_{i=1}^{N} d_i||e_i|| \leq c_M\gamma\Delta_M\sqrt{N}\varsigma||e|| \tag{3.2}$$

Therefore, with the new definition of $\beta = c_M(kr_M + \gamma\Delta_M\sqrt{N}) > 0$, we still get to inequality (2.15), which thanks to Hypothesis 3 can be rewritten as

$$\dot{\eta} \leq -\psi\eta + \beta\varsigma \tag{3.3}$$

From here we proceed as in Subsection 2.2.2, just having ψ instead of $c\lambda - L_f$, so that we end up with

$$\eta(t) \leq \left(\eta_0 + \frac{\beta k_\varsigma}{|\lambda_\varsigma - \psi|} \right) e^{-\lambda_c t} \tag{3.4}$$

which concludes the proof. In the unlikely event of $\psi = \lambda_\varsigma$, we can always reason as in Remark 6. □

3.4 Topology Requirements for Synchronization

Here we would like to make some considerations about how Hypothesis 3 can be fulfilled by acting on the parameters of the network, taking into consideration that this time the graph configuration is time-varying.

First of all, in order to satisfy Hypothesis 3 we need that $\lambda > 0$ at every time instant. This means that all the configurations assumed by the graph over time must be pinned, meaning that the considered topology must be switching pinned.

Assuming that the graph is always pinned, we also need that $c\lambda > L_f$ at all times. This can be obtained by using a control gain c that is large enough. It is easy to picture some criteria to calculate how large this gain shoud be.

With regard to this, let us indicate with $g(t)$ the augmented graph exhibited by network (1.4) at time t, and let us also indicate with $\hat{\mathcal{G}}$ the finite set of augmented graphs corresponding to all the possible configurations of the network that make the graph pinned. Moreover, let us introduce the lowest and the highest value assumed by the smallest eigenvalue of the augmented Laplacian when considering all the possible pinned graphs.

$$\lambda_m = \min_{g(t) \in \hat{\mathcal{G}}} \{\lambda(t)\} > 0, \qquad \lambda_M = \max_{g(t) \in \hat{\mathcal{G}}} \{\lambda(t)\} > 0 \tag{3.5}$$

The control gain c is strictly lower-bounded by $\frac{L_f}{\lambda_m} > 0$.

3.5 Absence of Zeno Behavior

Here we extend the proof of absence of Zeno behavior to the case of switching graphs. Again, we use the very same passages as in the static case, but due to time-dependence of some graph parameters we end up with more conservative upper bounds.

Hypothesis 4. *Function f is globally Lipschitz with Lipschitz constant L_f and there exists a constant $\psi > \lambda_\varsigma$ such that the minimum eigenvalue λ of the augmented Laplacian of the network satisfies $c\lambda > L_f + \psi$ for all $t \geq 0$.*

Theorem 4. *Under Hypothesis 4 the time sequences $\{t_k^i\}$ with $i = 1 \ldots N$ do not exhibit Zeno behavior.*

Proof. Following the passages in Subsection 2.4.1, we start off by observing that, under Hypothesis 4, inequality (3.4) can be rewritten as

$$\eta(t) \leq \left(\eta_0 + \frac{\beta k_\varsigma}{\psi - \lambda_\varsigma} \right) e^{-\lambda_\varsigma t} \tag{3.6}$$

Therefore, defining $\chi = \frac{\eta_0}{k_\varsigma} + \frac{\beta}{\psi - \lambda_\varsigma} > 0$, we can bound again the error norm with

$$\eta \leq \chi\varsigma \qquad \forall t \geq 0 \tag{3.7}$$

Then we proceed as in Subsection 2.4.1, but instead of (2.29) and (2.30) we get the following inequalities that take the switchings into account.

$$c \sum_{j=1}^{N} a_{ij}(||e_{ij}|| + ||\tilde{e}_{ij}||) \leq c_M \gamma (2\chi + 1) \Delta_M \varsigma \tag{3.8}$$

$$ckp_i(||e_i|| + ||\tilde{e}_i||) \leq c_M k(\chi + 1)\varsigma \tag{3.9}$$

Therefore, instead of having a different ω_i for any of the nodes, we have a common value

$$\omega = L_f \chi + c_M \gamma (2\chi + 1) \Delta_M + c_M k(\chi + 1) > 0 \tag{3.10}$$

Therefore we conclude the first part of the proof with inequalities

$$||\dot{e}_i|| \leq \omega\varsigma \qquad ||\dot{e}_{iq}|| \leq 2\omega\varsigma \tag{3.11}$$

The second part of the proof goes as in Subsection 2.4.2, with $\omega_i = \omega_q = \omega$, and shows that after an agent violates condition (2.1), a finite time interval must pass before the same node violates it once again. This is not sufficient anymore to prove absence of Zeno behavior, since between two consecutive violations of conditions (2.1) more triggers may be generated because of the switchings. However, since two consecutive switchings involving the same node must be separated by a finite time $\tau_d > 0$, absence of Zeno behavior still holds. □

Remark 9. *In this case, absence of Zeno behavior does not imply also a finite inter-event time. Indeed, an instant after condition* (2.1) *is violated by a node, a switching that involves the same node may occur, generating two events that may be arbitrarily close. A way to have a finite inter-event time over a switching graph would be to impose that nodes do not accept to acquire new neighbors, or to be pinned, before a certain amount of time has passed after their last trigger. How realistic this assumption is depends on the considered application, but note that it poses a constraint only on the generation of new links and pins. Failures in the links and on the pinning feedback, which are less likely to be under control, can still occur arbitrarily close to other events, since they do not generate a trigger.*

3.6 Numerical Experiments

In this section we are going to present some numerical results obtained on a switching pinned topology scenario. In particular, we show that complete synchronization can be achieved with absence of Zeno behavior thanks to an appropriate choice of the control parameters.

In this experiment the starting network is made up of $N = 10$ identical Chua's oscillators described by (2.41) and with parameters defined as in (2.43), and the odds of an edge connecting two arbitrary nodes are worth 30%.

As interaction protocol and control protocol we choose $\Gamma = I_n$ and $K = 10I_n$, respectively. As for the parameters of the threshold function we choose $k_\varsigma = 0.05$ and $\lambda_\varsigma = 0.18$. As for the variations in the network topology, we have chosen a test-bed where $N_c = 50$ switchings occur at constant frequency during the simulation. Of course this means that a finite number of switchings occurs in a finite time. In this experiment each switching consists in selecting randomly a couple of nodes (i, j) with $i \neq j$, and changing their state of connection: if an edge exists between i and j then it is removed, otherwise it is created. We do not consider switchings causing accidental variations in the pinning matrix P. On the contrary, everytime a switching causing accidental variations in the graph Laplacian L occurs, we intentionally adjust the pinning matrix so that, with the minimum number of pin nodes, it holds that $\lambda(t) > \frac{L_f}{7.5} > 0$ for all $t \geq 0$. Then we choose a time-varying control gain worth $c(t) = \frac{\psi + L_f}{\lambda(t)}$ with $\psi = 0.5$, so that Hypothesis 4 is fulfilled. Finally, we choose initial conditions randomly.

Figures 3.1 and 3.2 show the trend of x_1 and e_1 during the simulation.

In Figures 3.3 and 3.4 we show some variables of interest with regard to the frequency of trigger events.

Figure 3.1: trend of the first state variable for nodes $i = 1 \ldots 10$ - switching topology scenario

(a) state

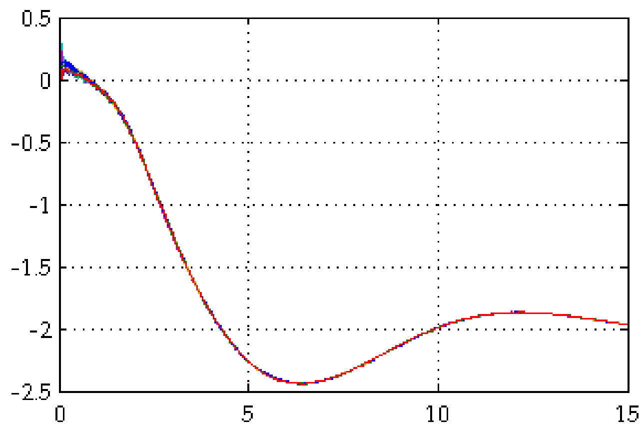

(b) state - zoom

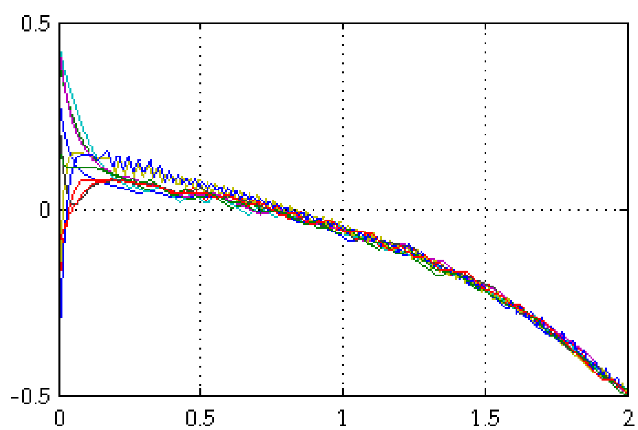

Figure 3.2: trend of the first error variable for nodes $i = 1 \ldots 10$ - switching topology scenario

(a) error

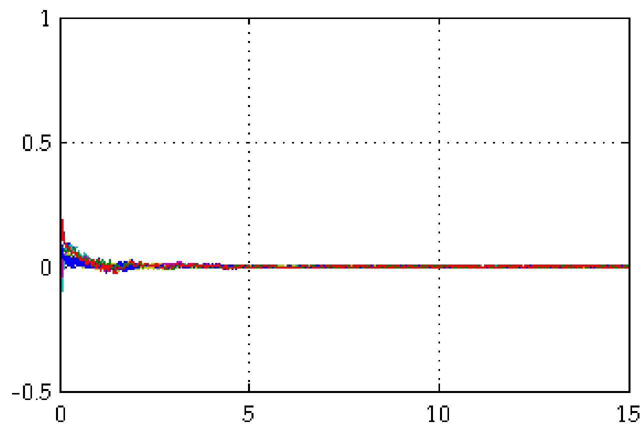

(b) error - zoom

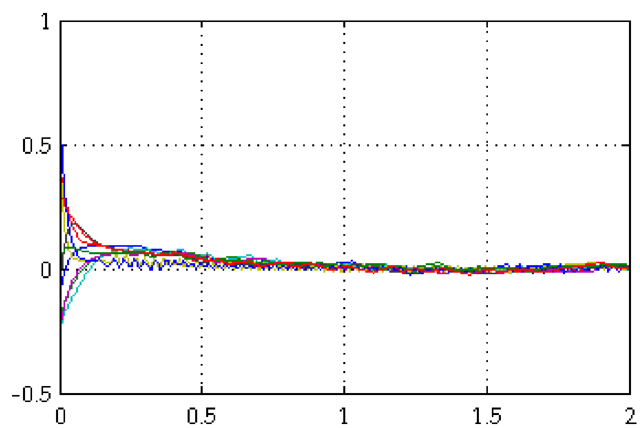

Figure 3.3: trigger events for nodes $i = 1 \dots 10$ - switching topology scenario

(a) first second of the simulation

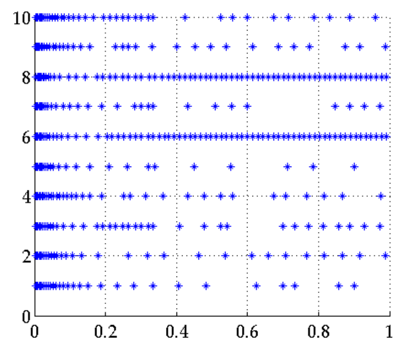

(b) last second of the simulation

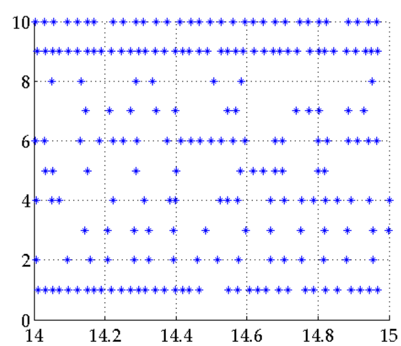

Figure 3.4: trend of the first control variable for nodes $i = 1 \dots 10$ - switching topology scenario

(a) control

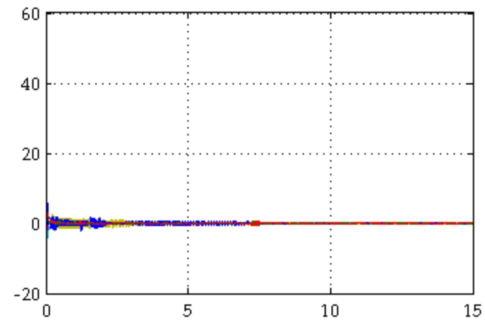

(b) control - zoom - first second of the simulation

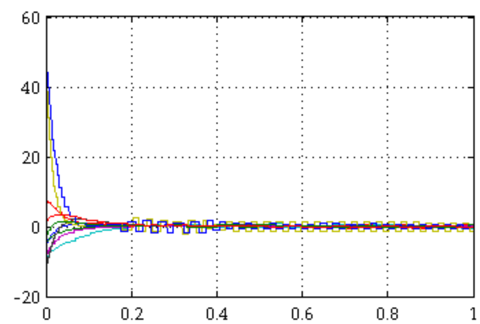

(c) control - zoom - last second of the simulation

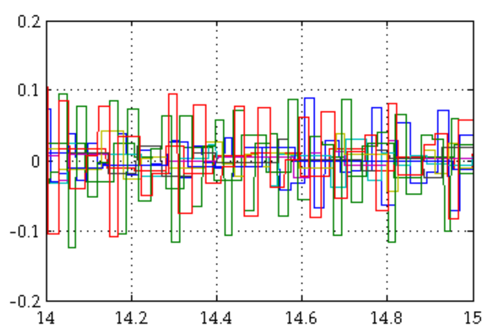

Chapter 4

Frequently Pinned Topologies

In this chapter we consider another particular class of networks with time-varying topologies and parameters, and we aim at individuating the hypotheses under which the results found for static topologies hold once again.

In Section 4.1 we give a simple description of this particular class of networks. In Section 4.2 we prove that, under opportune hypotheses, the control algorithm designed for switching topologies achieves the goal of complete synchronization also in this new scenario. In Section 4.3 we reflect on how these hypotheses can be fulfilled by acting on the parameters of the network. In Section 4.4 we prove that, under slightly more restrictive hypotheses, the time sequences defined in our algorithm do not exhibit Zeno behavior. Finally in Section 4.5 we describe the network that we have considered for numerical validation of our algorithm.

4.1 Definition of Frequently Pinned Topologies

In this section we would like to define time-varying networks whose graph is not always pinned. In other words, we assume that at some time instant there might be components of the network that do not contain any pin node. Nevertheless, we suppose that the amount of time in which the graph is not pinned is small enough for complete synchronization to be still achievable with absence of Zeno behavior for the trigger sequences. In order to address the described scenario, let us introduce a special class of switching graph, which we shall call *frequently pinned*.

Definition 4 (frequently pinned graph)**.** *A switching graph is said to be* frequently pinned *on a period $T > 0$ if, for any time $t \geq 0$, there exists a time $t^* \in [t, t+T)$ such that the graph is pinned at time t^*.*

Remark 10. *Thanks to the presence of a finite dwell time, it is easy to see that if a graph is frequently pinned then it holds that*

$$\int_t^{t+\hat{T}} \lambda(\tau)\ d\tau > 0 \tag{4.1}$$

for any $t \geq 0$ and $\hat{T} > T$. Conversely, if inequality (4.1) *holds for a certain value $\hat{T} > 0$, then the graph is frequently pinned on any period $T \geq \hat{T}$.*

4.2 Complete Synchronization

In this section we prove that, under opportune hypotheses, the control algorithm designed for switching topologies achieves the goal of complete synchronization. We also give a lower bound for the convergence rate of the error norm.

In particular we extend the proof of complete synchronization to the case of frequently pinned graphs. We start off by implementing the very same passages as in the static case.

Hypothesis 5. *Function f is one-side Lipschitz with Lipschitz constant L_f and the minimum eigenvalue λ of the augmented Laplacian of the network satisfies the following condition.*

$$\exists \psi > 0,\ \hat{T} > 0: \quad \frac{1}{\hat{T}} \int_t^{t+\hat{T}} (c\lambda - L_f) d\tau \geq \psi \tag{4.2}$$

Theorem 5. *Under Hypothesis 5, network* (1.4) *with control signal* (1.6) *and Update Rule 2 achieves complete synchronization as defined in* (1.5). *Morevoer, convergence to zero of the error norm is exponential with rate* $\lambda_c = \min\{\psi, \lambda_\varsigma\} > 0$.

Proof. The proof of this theorem is divided in two parts: in the former we prove that a particular sequence of the error norm is upper-bounded by a negative exponential, in the latter we use the previous result to prove that the error norm itself is upper-bounded by a negative exponential with the same rate of convergence. □

4.2.1 Upper Bound for a Sequence of the Error Norm

Reasoning in the same way as the case of a static topology, it is easy to see that inequality (2.15) still holds with the definition of $\beta = c_M(kr_M + \gamma\Delta_M\sqrt{N}) > 0$.

$$\dot{\eta}(t) \leq (L_f - c\lambda)\eta(t) + \beta\varsigma(t) \tag{4.3}$$

Integration of the previous inequality via Laplace's formula and application of the comparison lemma [61] yield

$$\eta(t+\hat{T}) \leq exp\left(\int_t^{t+\hat{T}} L_f - c(\tau)\lambda(\tau)\ d\tau\right)\eta(t)+$$
$$+\beta\int_t^{t+\hat{T}} exp\left(\int_\tau^{t+\hat{T}} L_f - c(\sigma)\lambda(\sigma)\ d\sigma\right)\varsigma(\tau)\ d\tau \tag{4.4}$$

Let us notice that the following equality holds $\forall\tau \in [t, t+\hat{T}]$.

$$\int_\tau^{t+\hat{T}} L_f - c\lambda\ d\sigma =$$
$$= \int_t^{t+\hat{T}} L_f - c\lambda\ d\sigma + \int_t^{\tau} c\lambda - L_f\ d\sigma \tag{4.5}$$

Therefore, taking into account the previous equality and taking advantage of Hypothesis 5, we can bound (4.4) with

$$\eta(t+\hat{T}) \leq exp(-\psi\hat{T})\eta(t)+$$

$$+\beta\int_t^{t+\hat{T}} exp(-\psi\hat{T})\ exp\left(\int_t^{\tau} c(\sigma)\lambda(\sigma) - L_f\ d\sigma\right)\varsigma(\tau)\ d\tau \tag{4.6}$$

The previous inequality can be rewritten as

$$\eta(t+\hat{T}) \leq exp(-\psi\hat{T})\ \cdot$$

$$\left[\eta(t) + \beta k_{\varsigma}\int_t^{t+\hat{T}} exp\left(\int_t^{\tau} c(\sigma)\lambda(\sigma)\ d\sigma - L_f(\tau-t) - \lambda_{\varsigma}\tau\right)d\tau\right]$$

$$\leq exp(-\psi\hat{T})\ \cdot$$

$$\left[\eta(t) + \beta k_{\varsigma}\ exp((L_f - c_M\lambda_M)t)\int_t^{t+\hat{T}} exp((c_M\lambda_M - L_f - \lambda_{\varsigma})\tau)d\tau\right] \tag{4.7}$$

For the sake of convenience let us define $\alpha = L_f + \lambda_{\varsigma} - c_M\lambda_M$ so that we can rewrite (4.7) as

$$\eta(t+\hat{T}) \leq e^{-\psi\hat{T}}\left[\eta(t) - \frac{\beta k_{\varsigma}}{\alpha}e^{(\alpha-\lambda_{\varsigma})t}e^{-\alpha t}(e^{-\alpha\hat{T}}-1)\right] =$$

$$= e^{-\psi\hat{T}}\left[\eta(t) + \frac{\beta k_{\varsigma}}{\alpha}e^{-\lambda_{\varsigma}t}(1-e^{-\alpha\hat{T}})\right] \tag{4.8}$$

Let us define now the following time sequence

$$\{t_h\}, h \in \mathbb{N}: \quad t_{h+1} - t_h = \hat{T} \tag{4.9}$$

and also $\eta(t_h) = \eta_h$, $\varsigma(t_h) = \varsigma_h$, $\tilde{\beta} = \frac{\beta k_{\varsigma}}{\alpha}(1-e^{-\alpha\hat{T}}) > 0$.

We can rewrite (4.8) as

$$\eta_{h+1} \leq \eta_h\ e^{-\psi\hat{T}} + \tilde{\beta}e^{-\psi\hat{T}}\ e^{-\lambda_{\varsigma}h\hat{T}} \qquad \forall h \in \mathbb{N} \tag{4.10}$$

Resolution of the recursive inequality yields

$$\eta_m \leq \eta_0 \ e^{-\psi m\hat{T}} + \tilde{\beta} e^{-\psi \hat{T}} \sum_{h=0}^{m-1} e^{-\lambda_\varsigma h\hat{T}} e^{-\psi(m-1-h)\hat{T}} =$$

$$= \eta_0 \ e^{-\psi m\hat{T}} + \tilde{\beta} \sum_{h=0}^{m-1} e^{-\lambda_\varsigma h\hat{T}} e^{-\psi(m-h)\hat{T}} =$$

$$= \eta_0 \ e^{-\psi m\hat{T}} + \tilde{\beta} e^{-\psi m\hat{T}} \sum_{h=0}^{m-1} e^{(\psi-\lambda_\varsigma)h\hat{T}} =$$

$$= \eta_0 \ e^{-\psi m\hat{T}} + \tilde{\beta} e^{-\psi m\hat{T}} \ \frac{1 - e^{(\psi-\lambda_\varsigma)m\hat{T}}}{1 - e^{(\psi-\lambda_\varsigma)\hat{T}}} =$$

$$= \eta_0 \ e^{-\psi m\hat{T}} + \tilde{\beta} \ \frac{e^{-\psi m\hat{T}} - e^{-\lambda_\varsigma m\hat{T}}}{1 - e^{(\psi-\lambda_\varsigma)\hat{T}}} \tag{4.11}$$

Therefore, if we define $\lambda_c = \min\{\psi, \lambda_\varsigma\} > 0$ we can bound (4.11) with

$$\eta_m \leq \eta_0 \ e^{-\psi m\hat{T}} + \tilde{\beta} \ \frac{e^{-\lambda_c m\hat{T}}}{|1 - e^{(\psi-\lambda_\varsigma)\hat{T}}|} \tag{4.12}$$

and of course, defining $\vartheta = \eta_0 + \frac{\tilde{\beta}}{|1-e^{(\psi-\lambda_\varsigma)\hat{T}}|} > 0$ as well, we get

$$\eta_m \leq \vartheta \ e^{-\lambda_c m\hat{T}} \tag{4.13}$$

With inequality (4.13) we conclude the first part of the proof, since sequence $\{\eta_h\}$ converges to zero exponentially with rate of convergence $\lambda_c > 0$.

4.2.2 Upper Bound for the Error Norm

Let us now examine what happens to the error norm itself $\eta(t)$ within the time interval $[t_h, t_{h+1})$. Taking into account that ς is a decreasing function, we can write

$$\dot{\eta} \leq (L_f - c\lambda) \ \eta + \beta \ \varsigma \leq L_f \ \eta + \beta \ \varsigma \leq L_f \ \eta + \beta \ \varsigma_0 \qquad \forall t \geq t_0 \tag{4.14}$$

Integration of the previous inequality via Laplace's formula and application of the comparison lemma [61] yield

$$\eta \leq e^{L_f(t-t_h)}\eta_h + \beta\varsigma_h \int_{t_h}^{t} e^{L_f(t-\tau)} d\tau =$$

$$= e^{L_f(t-t_h)}\eta_h + \beta e^{L_f t}\left(\int_{t_h}^{t} e^{-L_f\tau} d\tau\right)\varsigma_h =$$

$$= e^{L_f(t-t_h)}\eta_h + \frac{\beta}{L_f}\left(e^{L_f(t-t_h)} - 1\right)\varsigma_h$$

$$\leq e^{L_f\hat{T}}\eta_h + \frac{\beta}{L_f}\left(e^{L_f\hat{T}} - 1\right)\varsigma_h \qquad \forall t \in [t_h, t_{h+1}) \tag{4.15}$$

where the last inequality is true thanks to (4.9).

Taking advantage of (4.13), we can upper-bound (4.15) with

$$\eta \leq \vartheta\ e^{L_f\hat{T}}\ e^{-\lambda_c h\hat{T}} + \frac{\beta k_\varsigma}{L_f}\left(e^{L_f\hat{T}} - 1\right)e^{-\lambda_\varsigma h\hat{T}} \qquad \forall t \in [t_h, t_{h+1}) \tag{4.16}$$

Defining $\tilde{\vartheta} = \vartheta\ e^{L_f\hat{T}} + \frac{\beta k_\varsigma}{L_f}\left(e^{L_f\hat{T}} - 1\right) > 0$, we can bound (4.16) with

$$\eta \leq \tilde{\vartheta}\ e^{-\lambda_c h\hat{T}} \qquad \forall t \in [t_h, t_{h+1}) \tag{4.17}$$

Since $h\hat{T} = t_h \geq t - \hat{T}\ \forall t \in [t_h, t_{h+1})$, we can write

$$e^{-\lambda_c h\hat{T}} \leq e^{\lambda_c\hat{T}}\ e^{-\lambda_c t} \qquad \forall t \in [t_h, t_{h+1}), \quad \forall h \in \mathbb{N} \tag{4.18}$$

so that we can finally upper-bound (4.17) with

$$\eta(t) \leq \tilde{\vartheta}\ e^{\lambda_c\hat{T}}\ e^{-\lambda_c t} \qquad \forall t \geq 0 \tag{4.19}$$

which concludes the proof of complete synchronization.

Remark 11. *We have not considered explicitly the unlikely event of $\alpha = 0$. However, even in that case we can rewrite (4.7) as*

$$\eta(t+\hat{T}) \leq e^{-\psi\hat{T}} \left[\eta(t) + c_M \beta k_\varsigma \hat{T} e^{-\lambda_\varsigma t}\right] \tag{4.20}$$

Then, if we define

$$\tilde{\beta} = \beta k_\varsigma \hat{T} > 0 \tag{4.21}$$

inequality (4.10) *still holds and the proof can be carried out in the very same way.*

Remark 12. *We have not considered explicitly the unlikely event of* $\psi = \lambda_\varsigma$. *However, even in that case we can rewrite* (4.11) *as*

$$\eta_m = \eta_0 \; e^{-\lambda_\varsigma m\hat{T}} + m\tilde{\beta}e^{-\lambda_\varsigma m\hat{T}} \qquad \forall m \in \mathbb{N} \tag{4.22}$$

Since the linear function m *can be upper-bounded with any positive exponential, we still get an exponential convergence, with a rate of convergence arbitrarily close to* λ_ς. *Specifically, for any arbitrarily small* ϵ *such that* $0 < \epsilon < \lambda_\varsigma$, *we can write*

$$m\epsilon\hat{T} \leq e^{m\epsilon\hat{T}} \qquad \forall m \in \mathbb{N} \tag{4.23}$$

and consequently we can rewrite (4.12) *as*

$$\begin{aligned} \eta_m &\leq \eta_0 \; e^{-\lambda_\varsigma m\hat{T}} + \tilde{\beta}\frac{e^{m\epsilon\hat{T}}}{\epsilon\hat{T}} e^{-\lambda_\varsigma m\hat{T}} = \\ &= \eta_0 \; e^{-\lambda_\varsigma m\hat{T}} + \frac{\tilde{\beta}}{\epsilon\hat{T}} e^{-(\lambda_\varsigma - \epsilon)m\hat{T}} \\ &\leq \left(\eta_0 + \frac{\tilde{\beta}}{\epsilon\hat{T}}\right) e^{-(\lambda_\varsigma - \epsilon)m\hat{T}} \qquad \forall m \in \mathbb{N} \end{aligned} \tag{4.24}$$

Inequality (4.24) *proves that the sequence* $\{\eta_h\}$ *converges to zero exponentially with rate of convergence* $\lambda_\epsilon = \lambda_\varsigma - \epsilon$, *which is slower than* λ_ς, *yet arbitrarily close to it. The remaining part of the proof can be carried out in the very same way, but of course the rate of convergence of the error norm will be itself* λ_ϵ.

4.3 Topology Requirements for Synchronization

Here we would like to make some considerations about how Hypothesis 5 can be fulfilled by acting on the parameters of the network, taking into consideration that this time the graph configuration is again time-varying and not always pinned.

First of all, in order to satisfy Hypothesis 5 we need the graph to be frequently pinned on a period $\hat{T}$. Assuming that this can be guaranteed, let us then consider the worst case. In a time window worth $\hat{T}$ the network exhibits only one pinned topology for the lowest possible time, which is the dwell time τ_d, and the minimum eigenvalue of the augmented Laplacian assumes the lowest possible value as well, which is $\lambda_m > 0$. In such a scenario, Hypothesis 5 can be satisfied by choosing a control gain strictly lower-bounded by $\frac{\psi+L_f}{\lambda_m}\frac{\hat{T}}{\tau_d}$.

4.4 Absence of Zeno Behavior

Here we extend the proof of absence of Zeno behavior to the case of frequently pinned graphs.

Hypothesis 6. *Function f is globally Lipschitz with Lipschitz constant L_f and the minimum eigenvalue λ of the augmented Laplacian of the network satisfies the following condition.*

$$\exists \psi > \lambda_\varsigma,\ \hat{T} > 0: \quad \frac{1}{\hat{T}} \int_t^{t+\hat{T}} (c\lambda - L_f) d\tau \geq \psi \tag{4.25}$$

Theorem 6. *Under Hypothesis 6 the time sequences $\{t_k^i\}$ with $i = 1 \dots N$ do not exhibit Zeno behavior.*

Proof. Under Hypothesis 6, equation (4.17) can be rewritten as

$$\eta(t) \leq \tilde{\vartheta}\ e^{-\lambda_\varsigma h \hat{T}} \qquad \forall t \in [t_h, t_{h+1}) \tag{4.26}$$

which, reasoning in the same way as in Theorem 5, leads to

$$\eta(t) \leq \tilde{\vartheta}\ e^{\lambda_\varsigma \hat{T}}\ e^{-\lambda_\varsigma t} \qquad \forall t \geq 0 \tag{4.27}$$

or equivalently, defining $\chi = \frac{\tilde{\vartheta}\ e^{\lambda_\varsigma \hat{T}}}{k_\varsigma} > 0$, to

$$\eta \leq \chi\ \varsigma \qquad \forall t \geq 0 \tag{4.28}$$

From this point on, the proof of absence of Zeno behavior is analogous to the one already carried out in the case of a switching pinned topology. □

4.5 Numerical Experiments

In this section we are going to present some numerical results obtained on a frequently pinned topology scenario. In particular, we show that complete synchronization can be achieved with absence of Zeno behavior thanks to an appropriate choice of the control parameters.

In this experiment the starting network is made up of $N = 10$ identical Chua's oscillators described by (2.41) and with parameters defined as in (2.43), and the odds of an edge connecting two arbitrary nodes are worth 30%.

As for the variations in the network topology, we have chosen a test-bed where $N_c = 50$ switchings occur at constant frequency during a simulation whose duration is worth $t_m = 15s$. In particular we have considered a scenario in which the incidence matrix and the pinning matrix periodically change during the simulation among $W = 5$ possible configurations, just one of which gives rise to a pinned topology. This means that the network exhibits a pinned topology every $T = 1.5s$. We have chosen a scenario in which the number r of pin nodes varies from 1 to 3.

As interaction protocol and control protocol we choose $\Gamma = I_n$ and $K = 10I_n$, respectively. As for the parameters of the threshold function, we choose $k_\varsigma = 0.025$ and $\lambda_\varsigma = 0.18$.

Since the switchings affecting the network are periodical and each topology shown by network has the same duration of $\frac{T}{W} = 0.3s$, Hypothesis 6 can be satisfied by choosing a constant control gain c at least worth $\frac{(\psi+L_f)W}{\hat{\lambda}}$, where $\hat{\lambda}$ represents the minimum eigenvalue of the augmented Laplacian for the only pinned topology in the experiment.

Specifically, since in our simulation $\hat{\lambda} \simeq 0.82$, we have chosen $\psi = 0.2$ so that so that Hypothesis 6 is satisfied with a constant control gain worth $c = 25$. Finally, we choose initial conditions randomly.

Figures 4.1 and 4.2 show the trend of x_1 and e_1 and u_1 during the simulation.

In Figures 4.3 and 4.4 we show some variables of interest with regard to the frequency of trigger events.

Figure 4.1: trend of the first state variable for nodes $i = 1 \ldots 10$ - frequently pinned topology scenario

(a) state

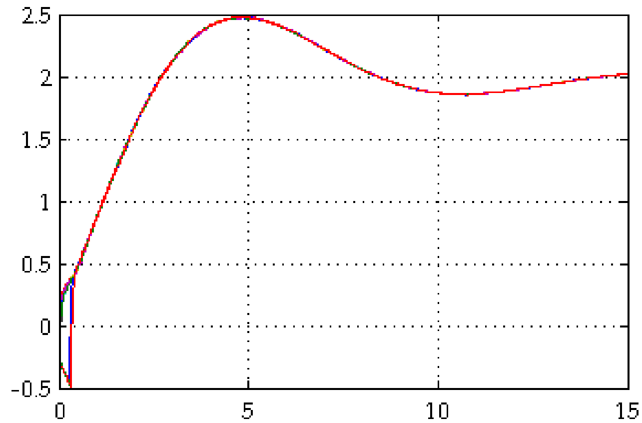

(b) state - zoom

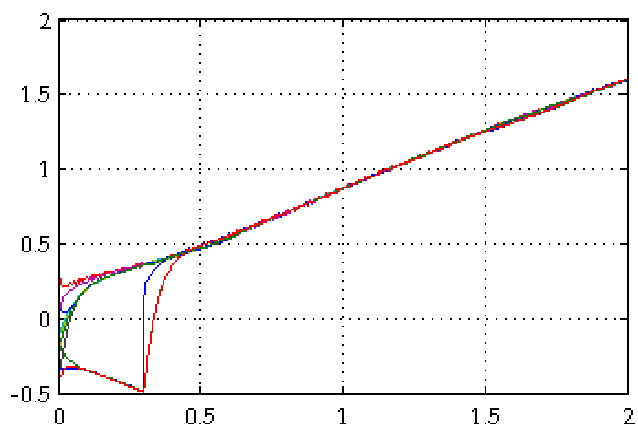

Figure 4.2: trend of the first error variable for nodes $i = 1 \dots 10$ - frequently pinned topology scenario

(a) error

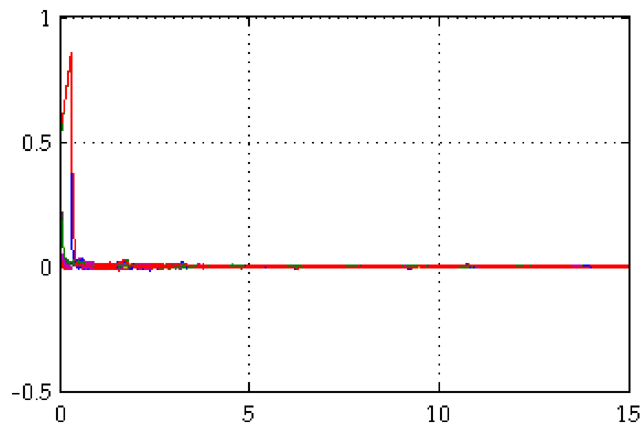

(b) error - zoom

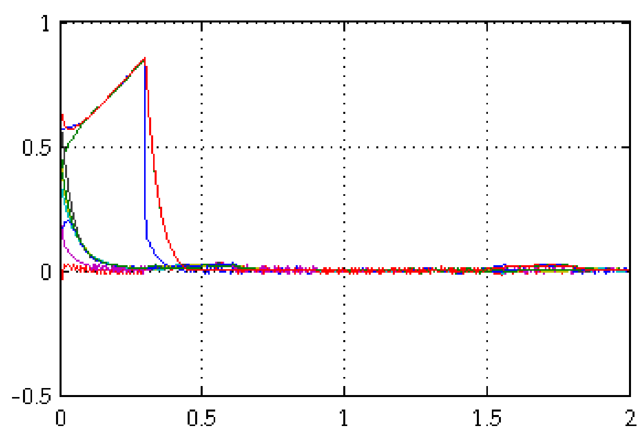

Figure 4.3: trigger events for nodes $i = 1 \dots 10$ - frequently pinned topology scenario

(a) first second of the simulation

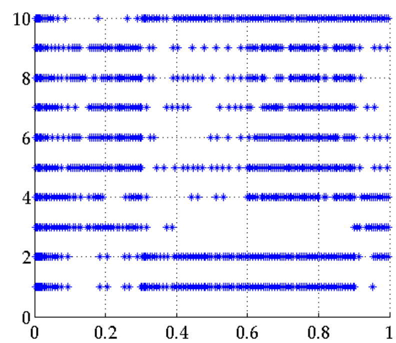

(b) last second of the simulation

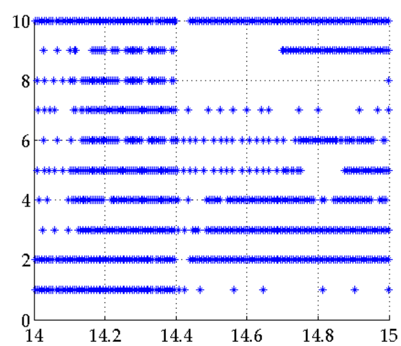

Figure 4.4: trend of the first control variable for nodes $i = 1 \dots 10$ - frequently pinned topology scenario

(a) control

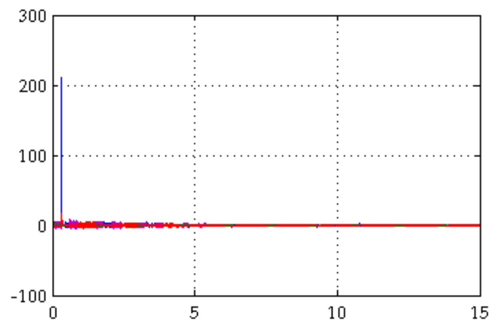

(b) control - zoom - first second of the simulation

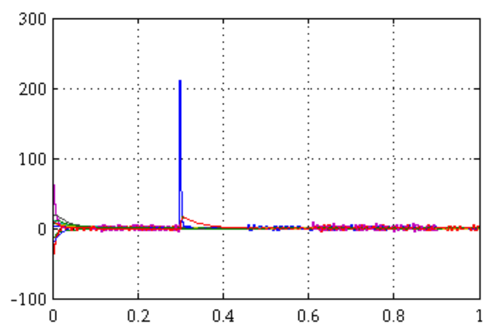

(c) control - zoom - last second of the simulation

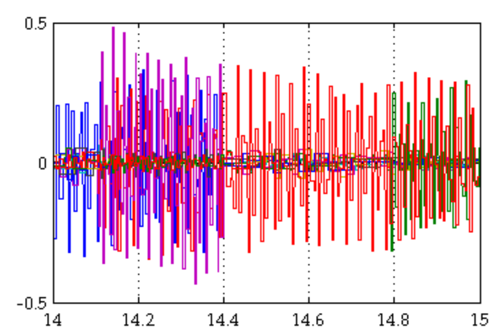

Chapter 5

Numerical Experiments on Fundamental Static Topologies

In this chapter we are going to present some numerical results obtained over fundamental static topologies in terms of the rate of convergence for the error norm. In particular we will show how the pin choice influences such a speed for a network made up of N identical Chua's oscillators.

In all the experiments we choose $k_\varsigma = 0.1$, $\lambda_\varsigma = 0.5$, $\Gamma = I_n$ and $K = p\ I_n$. The number of nodes r, the control gain c and the control strength $k = p$ are chosen so that Hypothesis 1 is fulfilled. This means that in all the following results complete synchronization is always guaranteed.

In Sections 5.1, 5.2, 5.3 and 5.4 we consider complete graph, star graph, path graph and ring graph respectively.

Figure 5.1: error norm - complete graph - $N = 10$, $c = 10$

(a) $r = 1$, $p = 10$

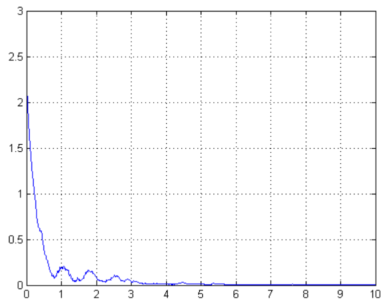

(b) $r = 1$, $p = 50$

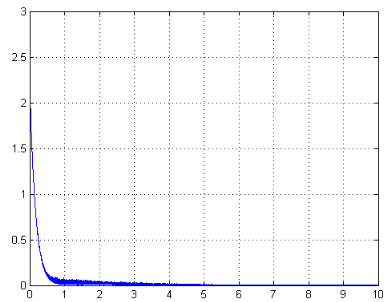

(c) $r = 3$, $p = 10$

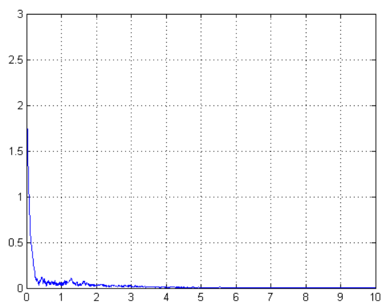

(d) $r = 3$, $p = 50$

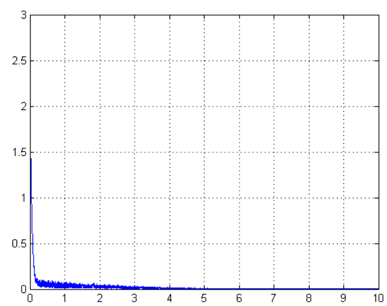

5.1 Complete Graph

In this section we are going to present some numerical results obtained over a complete graph.

Figure 5.1 shows the trend of the error norm for different values of the number of nodes r and the control strength p.

Figure 5.2 shows the comparison between the trends of the error norm obtained in two different scenarios: in the first case we suppose $p = 10$ and we compare the trends obtained for $r = 1$ and $r = 3$, while in the second case we suppose $p = 50$ and we compare the trends obtained again for $r = 1$ and $r = 3$.

Figure 5.2: error norm comparison - complete graph - $N = 10$, $c = 10$

(a) p=10

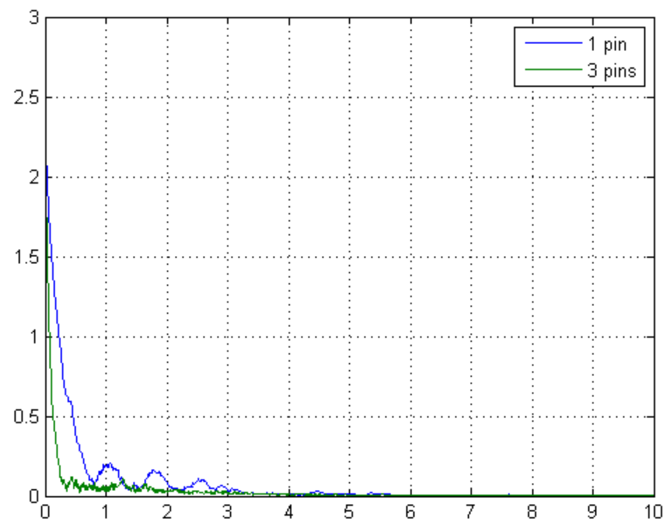

(b) p=50

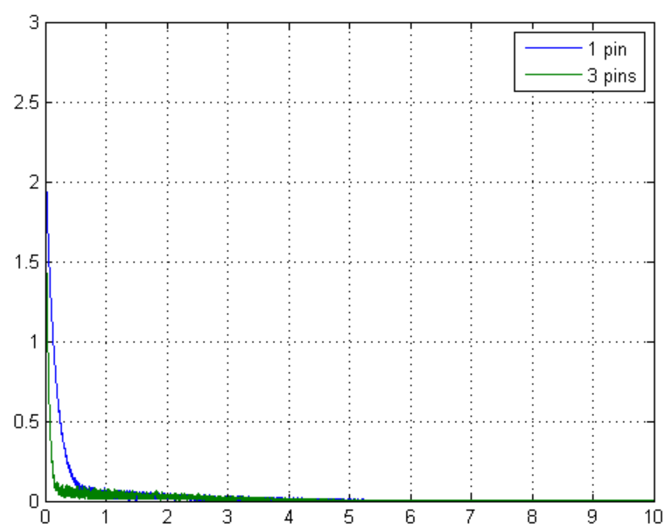

5.2 Star Graph

In this section we are going to present some numerical results obtained over a star graph.

Figure 5.3 shows the trend of the error norm when pinning just one node in two different scenarios: the former when the pin is the central node, the latter when the pin is a peripheral node. Figure 5.4 shows the comparison between these two trends.

Figure 5.5 shows the trend of the error norm in two different scenarios when pinning $m \leq \frac{N}{2}$ nodes: the former when the central node and $m-1$ peripheral nodes are pinned, the latter when the m pin nodes are all peripheral. Figure 5.6 shows the comparison between these two trends. As we expected, the trend of the error norm when pinning also the central node is better.

Figure 5.7 shows the comparison between the trends of the error norm obtained in two different scenarios when pinning $m > \frac{N}{2}$ nodes and choosing a control strength p so that the minimum eigenvalue λ of the augmented Laplacian is lower than $\frac{2m-N}{m-1}$: in the first case we suppose that the m pin nodes are all peripheral, while in second case we suppose that the central node and $m-1$ peripheral nodes are pinned. As we expected, the trend of the error norm when pinning only peripheral nodes is better.

Figure 5.8 shows the comparison between the trends of the error norm obtained in two different scenarios when pinning $m > \frac{N}{2}$ nodes and choosing a control strength p so that the minimum eigenvalue λ of the augmented Laplacian is greater than $\frac{2m-N}{m-1}$: in the first case we suppose that the m pin nodes are all peripheral, while in second case we suppose that the central node and $m-1$ peripheral nodes are pinned. As we expected, the trend of the error norm when pinning also the central nodes is better.

Figure 5.9 shows the comparison between the trends of the error norm obtained in two different scenarios when pinning $m = N-1$ nodes: in the first case we suppose that all the $N-1$ peripheral nodes are pinned, while in second case we suppose that the central node and $N-2$ peripheral nodes are pinned.

Figure 5.3: error norm - star graph - $N = 10$, $r = 1$, $c = 50$, $p = 10$

(a) central node

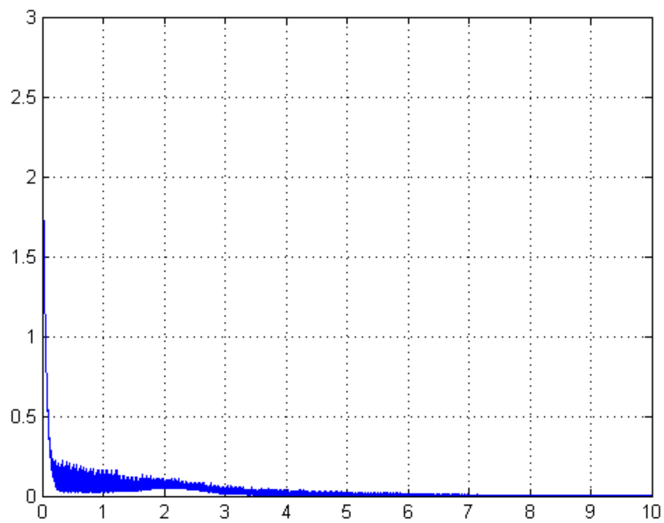

(b) peripheral

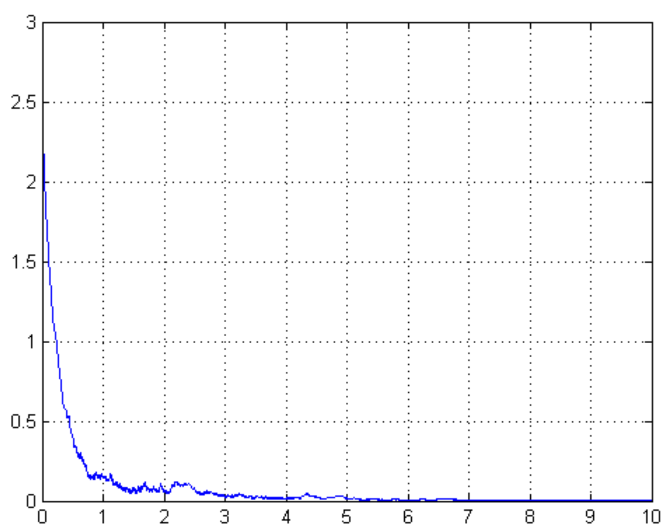

Figure 5.4: error norm comparison - star graph - $N = 10$, $r = 1$, $c = 50$, $p = 10$

(a) comparison

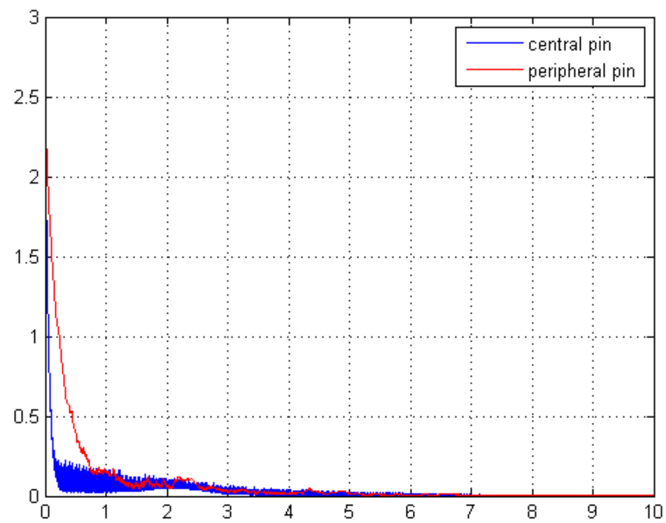

(b) zoom

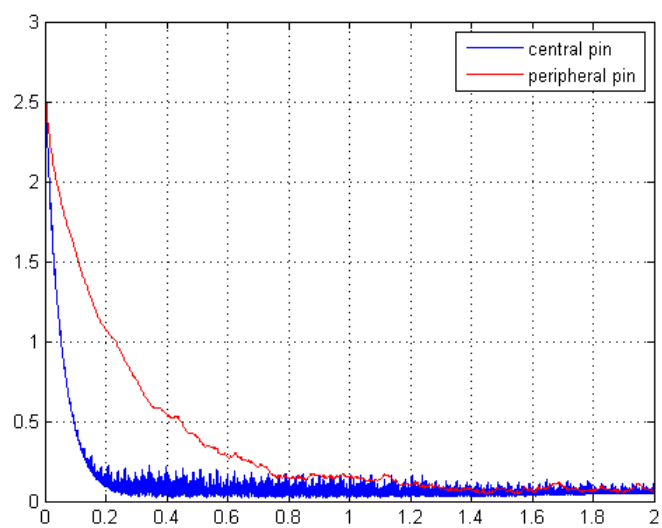

Figure 5.5: error norm - star graph - $N = 10$, $r = 3$, $c = 20$, $p = 10$

(a) central + peripheral

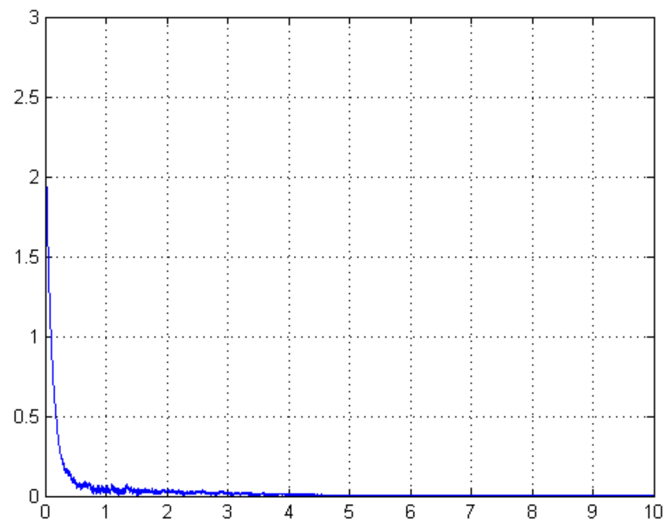

(b) all peripheral

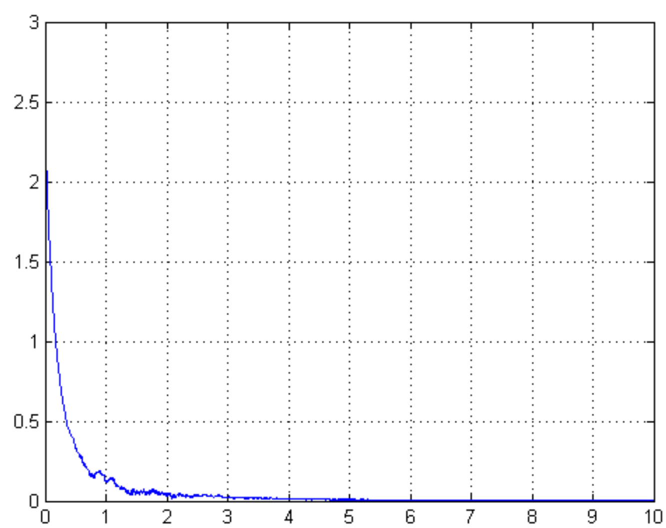

Figure 5.6: error norm comparison - star graph - $N = 10$, $r = 3$, $c = 20$, $p = 10$

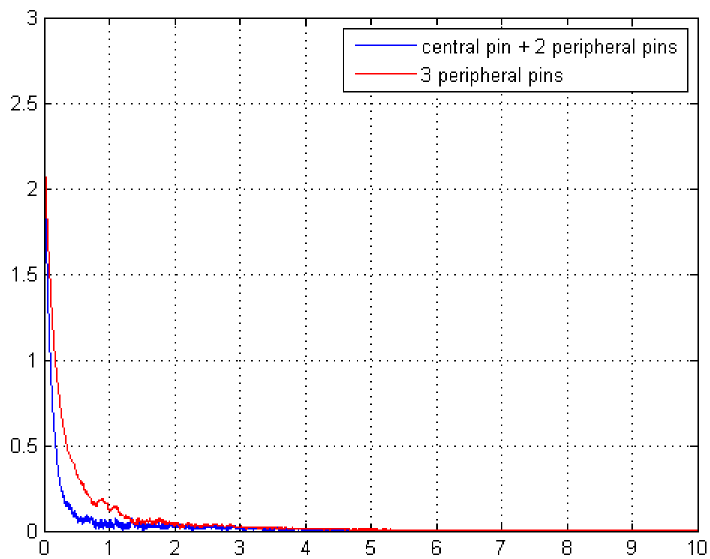

As we expected, the trend of the error norm when pinning only peripheral nodes is better.

5.3 Path Graph

In this section we are going to present some numerical results obtained over a path graph.

Figure 5.10 shows the trend of the error norm in three different scenarios when pinning just one node: in the first case the first node is pinned, in the second case the second node is pinned while in the last case the central node is pinned. Figure 5.11 shows the comparison between these three trends. As we expected, the further the pin is from the periphery, the better the trend of the error norm gets.

Figure 5.12 shows the trend of the error norm in two different scenarios: in the first case the central node is pinned with double control strength $p = 20$, in

Figure 5.7: error norm comparison - star graph - $N = 10$, $r = 6$, $c = 20$, $p = 0.5$, $\lambda < \frac{2m-N}{m-1}$

(a) comparison

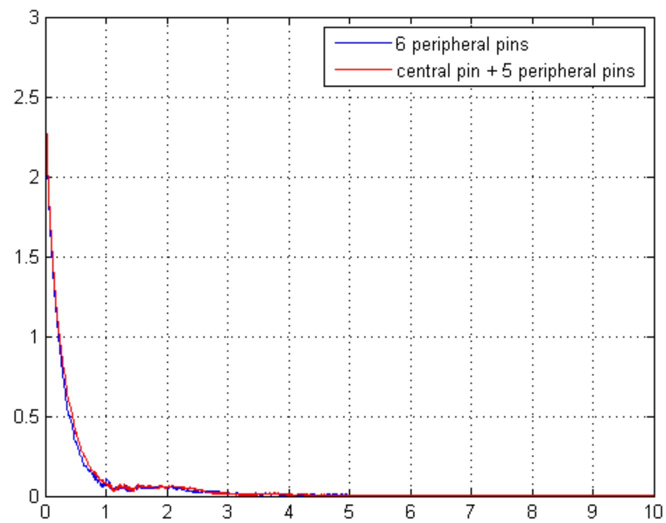

(b) zoom

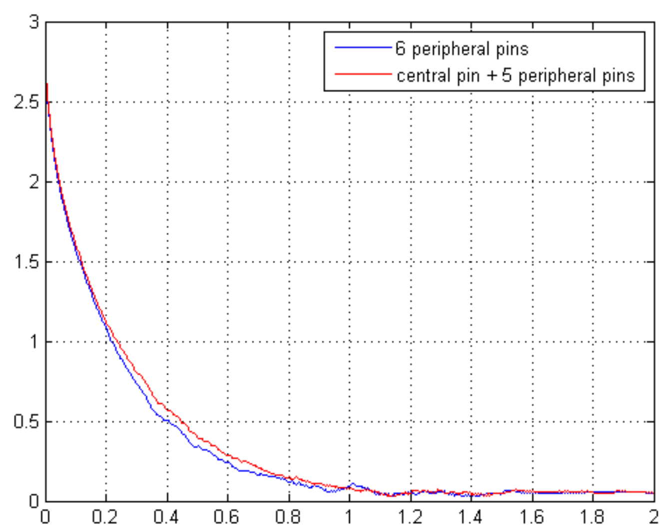

Figure 5.8: error norm comparison - star graph - $N = 10$, $r = 6$, $c = 20$, $p = 5$, $\lambda > \frac{2m-N}{m-1}$

(a) comparison

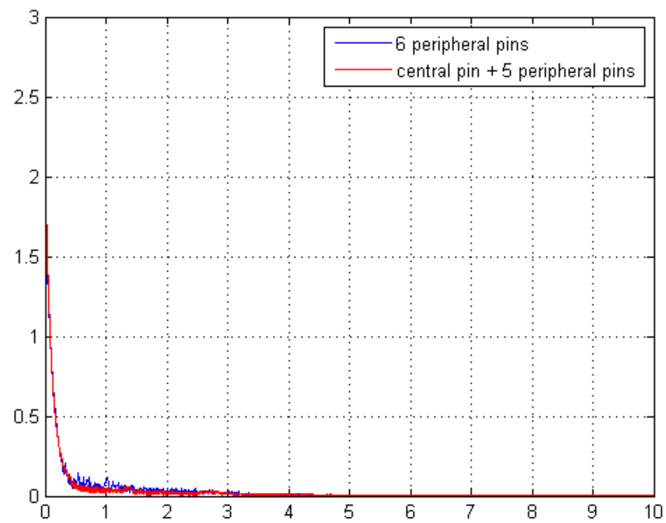

(b) zoom

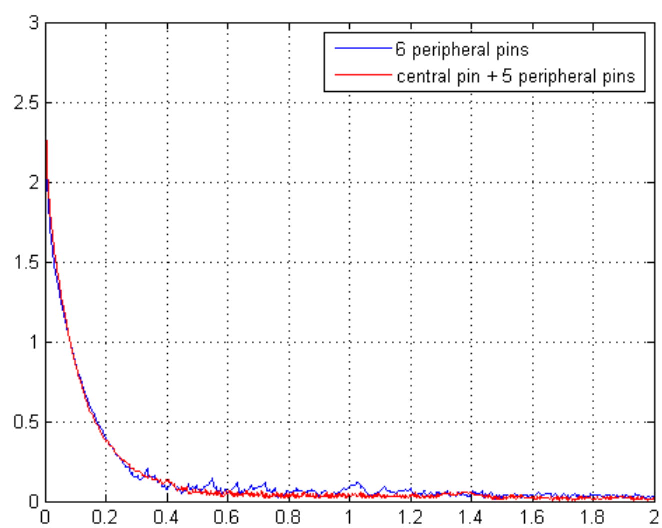

Figure 5.9: error norm comparison - star graph - $N = 10$, $r = 9$, $c = 10$, $p = 5$

(a) comparison

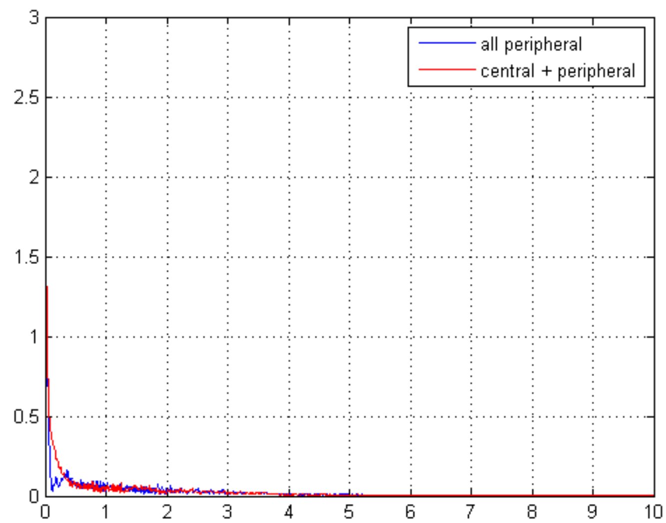

(b) zoom

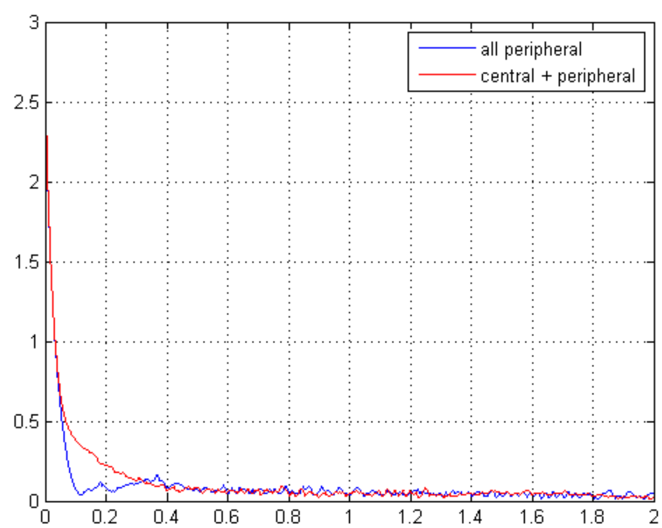

Figure 5.10: error norm - path graph - $N = 9$, $r = 1$, $c = 150$, $p = 10$

(a) first node

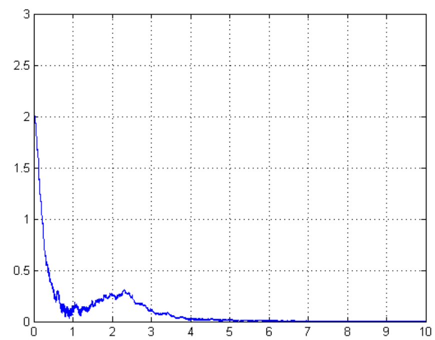

(b) second node

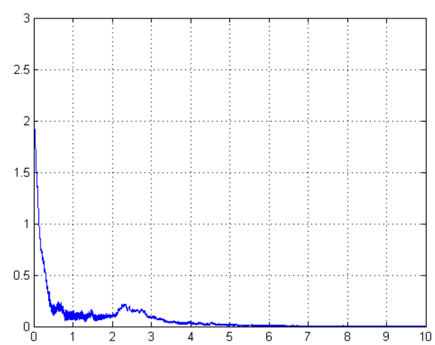

(c) central node

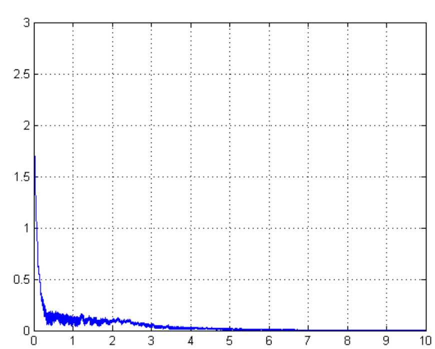

Figure 5.11: error norm comparison - path graph - $N = 9$, $r = 1$, $c = 150$, $p = 10$

(a) comparison

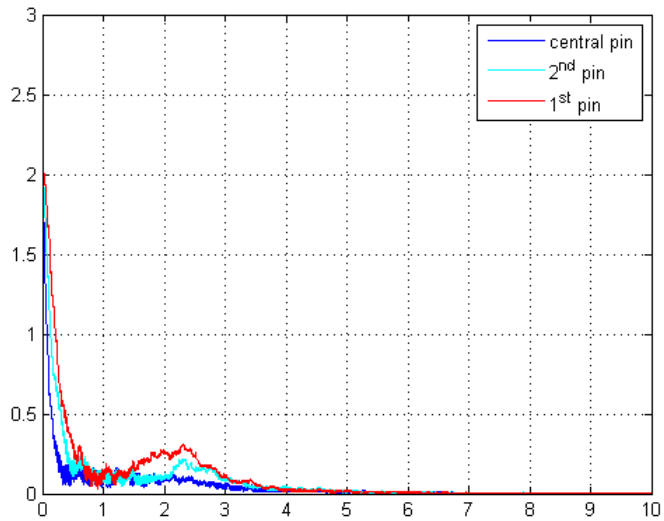

(b) zoom

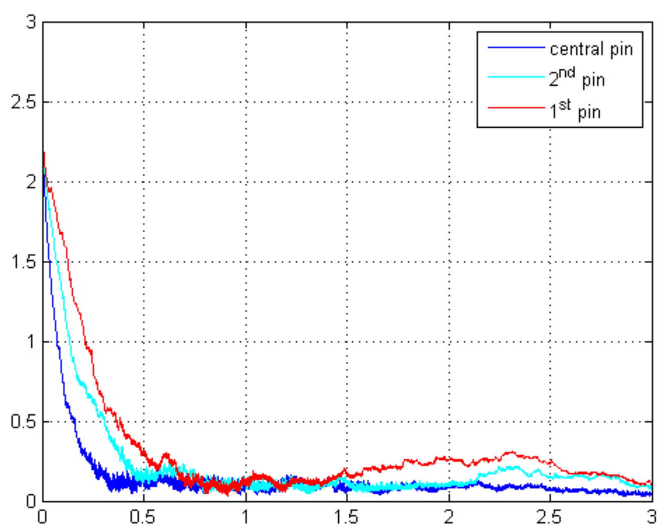

Figure 5.12: error norm comparison - path graph - $N = 9$, $c = 150$

(a) comparison

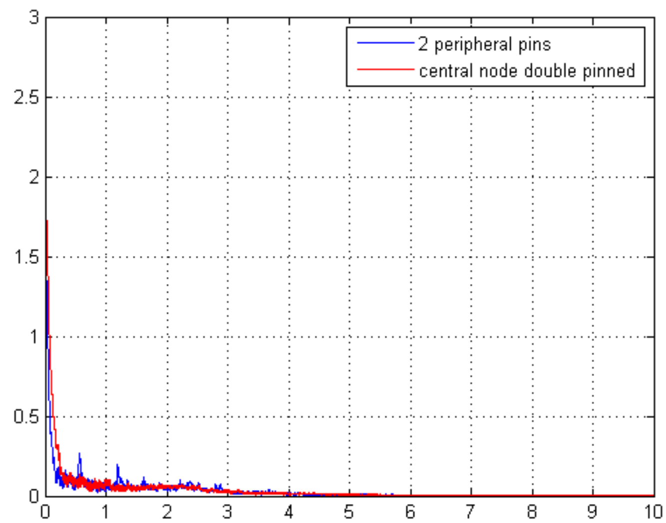

(b) zoom

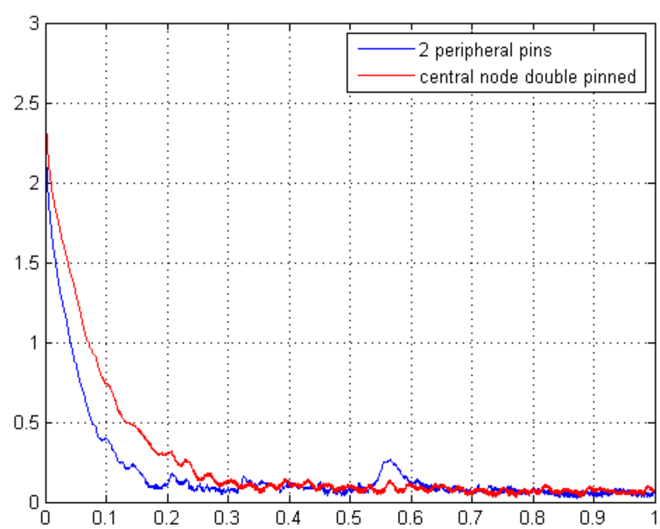

the second case the two peripheral nodes are both pinned, each one with control strength $p = 10$. Figure 5.11 shows the comparison between these two trends. As we expected, the trend of the error norm when pinning both the peripheral nodes is better.

5.4 Ring Graph

In this section we are going to present some numerical results obtained over a ring graph.

Figure 5.13 shows the trend of the error norm when pinning just one node in two different scenarios: the former when $p = 10$, the latter when $p = 50$. Figure 5.14 shows the comparison between these two trends. As we expected, the greater the control strength p, the better the trend of the error norm.

Figure 5.15 shows the trend of the error norm in three different scenarios: in the first case just one node is pinned with double control strength $p = 10$, in the second case two consecutive nodes are pinned, each one with control strength $p = 5$, and finally in the last case two symmetrical nodes are pinned, each one again with control strength $p = 5$. As we expected, the trend of the error norm when pinning two consecutive nodes is better than when pinning just one node with double strength. Moreover, the trend of the error norm when pinning two symmetrical nodes is better than when pinning two consecutive nodes.

Figure 5.13: error norm - ring graph - $N = 10$, $r = 1$, $c = 50$

(a) $p = 10$

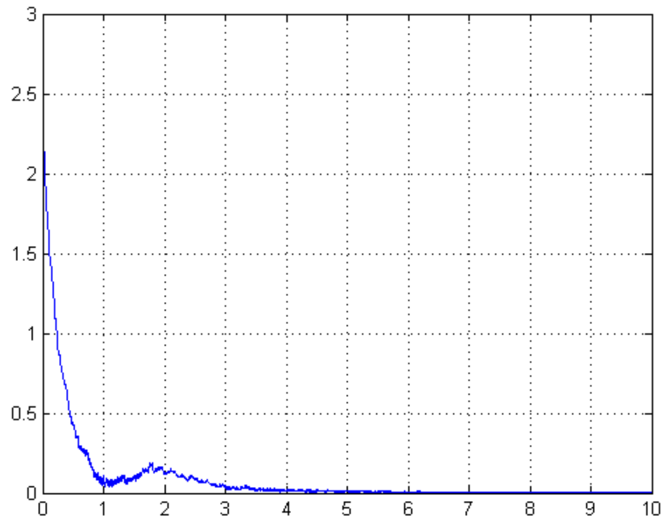

(b) $p = 50$

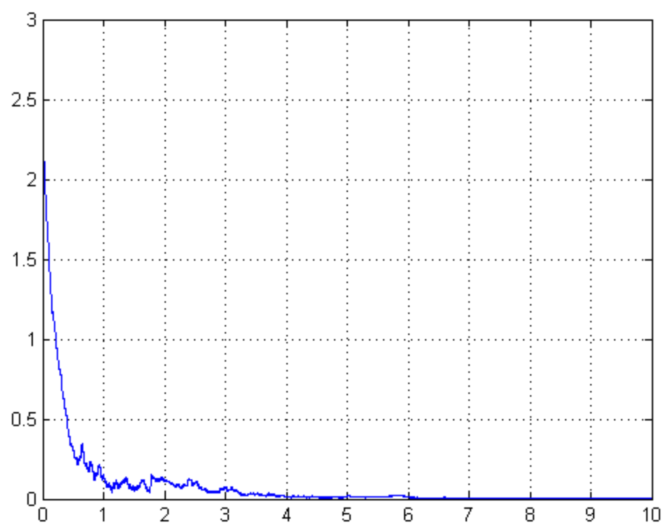

Figure 5.14: error norm comparison - ring graph - $N = 10$, $r = 1$, $c = 50$

(a) comparison

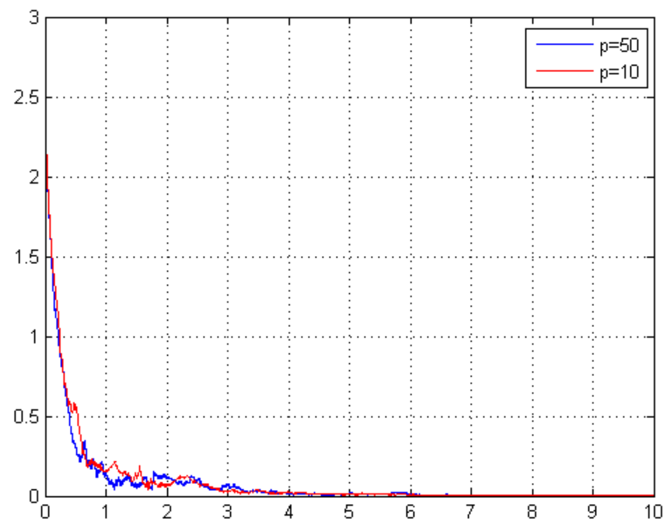

(b) zoom

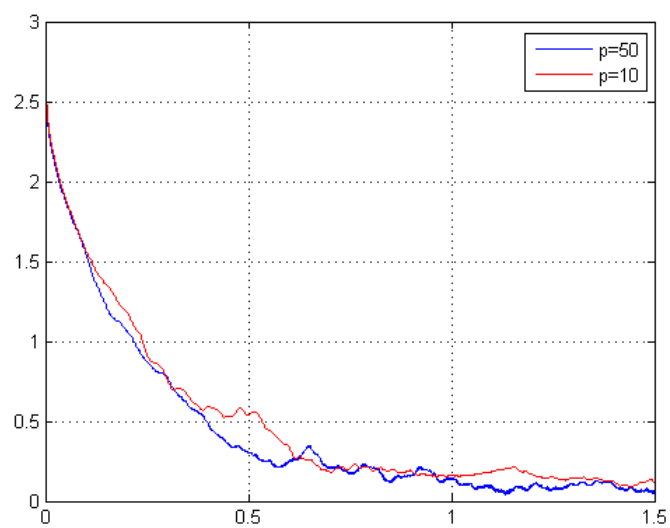

Figure 5.15: error norm comparison - ring graph - $N = 8$, $c = 50$

(a) comparison

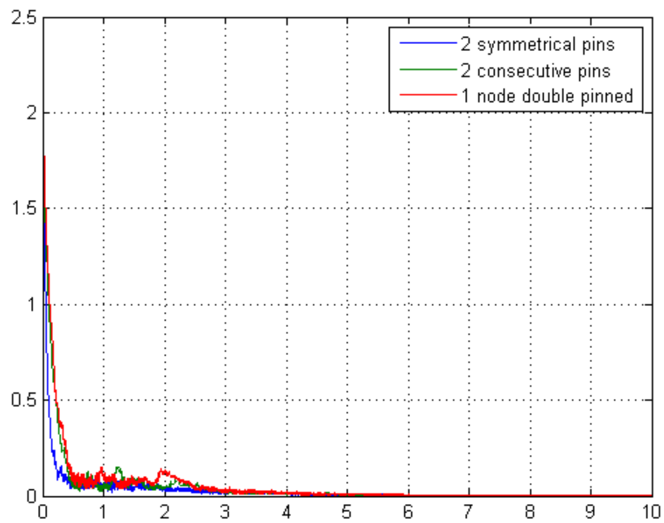

(b) zoom

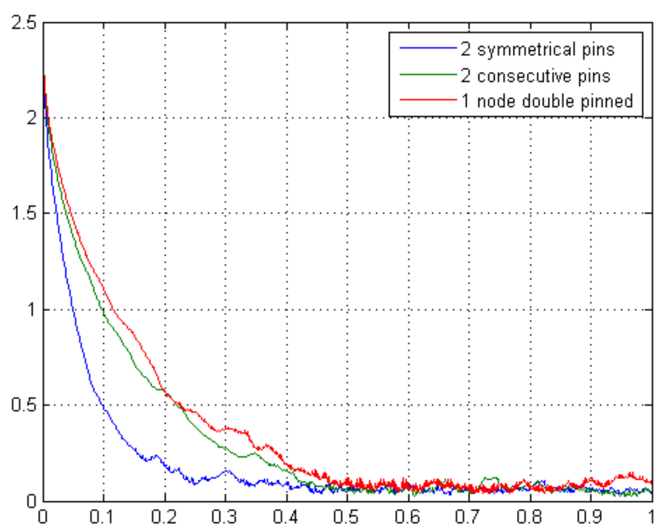

Chapter 6

Conclusions

This chapter concludes the master thesis with a short summary of our results and an overview of possible extensions and future developments.

6.1 Main Results Summary

In this master thesis we have presented an algorithm for distributed event-triggered pinning control on a network of identical nonlinear oscillators. In order to address the pinning control problem specifically, the augmented graph formalism has been introduced. Moreover, the concepts of pinned, switching pinned and frequently pinned topologies have been introduced as an extension of the concepts of connected, switching connected and slow switching topologies respectively. Complete synchronization and absence of Zeno behavior have been proven for each of the considered topologies. A finite inter-event time between two consecutive triggers of the same time sequence has been guaranteed for pinned topologies. Numerical experiments confirming the theoretical results have been presented.

6.2 Future developments

Pinning control is a relatively newborn branch of automation and a pinning control theory is in process of formation. Distributed event-triggered control has been widely addressed in recent papers, but only a small part of them has dealt with nonlinear oscillators so far. Therefore a large set of open questions and possibilities for future developments can be outlined from the presented work. Here we list some points which could be interesting to address.

- First of all, networks whose topology cannot be described as frequently pinned may be studied. Some interesting results in this direction can be found in [62], where sufficient conditions for local pinning controllability of a switching network of nonlinear agents under time-continuous control are derived analytically. Such sufficient conditions relate to the frequency of the switchings and to the eigenvalues of the augmnted laplacian of an averaged topology, but do not require that the network be frequently pinned. Of course these results may serve as an important source of inspiration if our analysis were to be extended to a more general class of switching topologies, but in our case global controllability should be investigated and event-triggered control laws should be considered.

- All our models consists of unweighed and undirected graphs. Weighted and/or directed graphs may be considered as network topologies. In fact, some of the properties that we use in our proofs rely on the symmetry of the Laplacian, which is lost in the case of a directed graph.

- The topologies we have taken into account are made up of identical nonlinear oscillators. Networks with heterogeneous agents may be considered instead.

- The networks that we have taken into account are made up of nonlinear oscillators whose model is perfectly known. Uncertainties in the model for the agents' dynamics may be considered instead.

- Delays in the agents' dynamics or in the communication protocol may be considered.
- In order to address more severe limitations on the capacity of the communication channels, a self-triggered algorithm may be designed for the examined topologies.

Appendix A

Topology Requirements for Positive Definiteness of the Augmented Laplacian

In this appendix we would like to find the topology requirements that an augmented graph has to satisfy for its augmented Laplacian to be positive definite.

Theorem 7. *The augmented Laplacian of an augmented graph is positive definite if and only if the graph is pinned.*

Proof. Without loss of generality, let us suppose that network (1.4) is made up of M connected components and let us suppose that nodes belonging to the same component correspond to consecutive entries of the graph Laplacian. Therefore L can be written as a block-diagonal matrix, with each block corresponding to one of the connected components. For convenience, let us also write matrix P as a block-diagonal matrix made up of M blocks, each one corresponding to one component of the network.

$$L = \begin{bmatrix} L_1 & & & \\ & L_2 & & \\ & & \ddots & \\ & & & L_M \end{bmatrix}, \qquad P = \begin{bmatrix} P_1 & & & \\ & P_2 & & \\ & & \ddots & \\ & & & P_M \end{bmatrix} \tag{A.1}$$

Note that different blocks might have different dimensions, each equal to the number of nodes in the corresponding component. We shall indicate such dimensions with M_i $\forall i = 1 \ldots M$.

Let us now define the two following matrices.

$$\hat{L} = L \otimes \Gamma = \begin{bmatrix} L_1 \otimes \Gamma & & & \\ & L_2 \otimes \Gamma & & \\ & & \ddots & \\ & & & L_M \otimes \Gamma \end{bmatrix} \tag{A.2}$$

$$\hat{P} = P \otimes K = \begin{bmatrix} P_1 \otimes K & & & \\ & P_2 \otimes K & & \\ & & \ddots & \\ & & & P_M \otimes K \end{bmatrix} \tag{A.3}$$

Note that matrix $\hat{L}$ is still a symmetric and positive semidefinite matrix, therefore we can individuate a basis of $\mathbb{R}_{Nn}$ made up of its unity-norm eigenvectors.

Let us write the generic vector $x \in \mathbb{R}_{Nn}$ as a linear combination of such eigenvectors

$$x = \sum_{i=1}^{N} \sum_{j=1}^{n} \alpha_{ij} v_i \otimes w_j \tag{A.4}$$

and let us use this expression to evaluate

$$\hat{L}x = \sum_{i=1}^{N} \sum_{j=1}^{n} \alpha_{ij} \hat{L} v_i \otimes w_j = \sum_{i=1}^{N} \sum_{j=1}^{n} \alpha_{ij} \lambda_i \mu_j v_i \otimes w_j \tag{A.5}$$

where v_i is the eigenvector of the graph Laplacian L corresponding to its i-th eigenvalue λ_i, and w_j is the eigenvector of the interaction protocol Γ corresponding to its j-th eigenvalue μ_j.

Since the graph Laplacian L has M components, eigenvalues λ_i are null for all $i = 1 \dots M$, and consequently

$$\hat{L}x = \sum_{i=M+1}^{N} \sum_{j=1}^{n} \alpha_{ij} \lambda_i \mu_j v_i \otimes w_j \tag{A.6}$$

Now let us evaluate

$$x^T \hat{L} x = \sum_{h=1}^{N} \sum_{k=1}^{n} \alpha_{hk} (v_h \otimes w_k)^T \sum_{i=M+1}^{N} \sum_{j=1}^{n} \alpha_{ij} \lambda_i \mu_j v_i \otimes w_j \tag{A.7}$$

Since $\hat{L}$ is a symmetric and positive semidefinite matrix, eigenvectors corresponding to different eigenvalues are orthogonal to each other. Therefore

$$x^T \hat{L} x = \sum_{i=M+1}^{N} \sum_{j=1}^{n} \alpha_{ij}^2 \lambda_i \mu_j ||v_i \otimes w_j||^2 = \sum_{i=M+1}^{N} \sum_{j=1}^{n} \alpha_{ij}^2 \lambda_i \mu_j \tag{A.8}$$

Since the eigenvalues λ_i and μ_j in equation (A.8) are strictly positive, the previous quantity is strictly positive itself, unless $\alpha_{ij} = 0 \ \forall i = M+1 \dots N, \forall j = 1 \dots n$.

If this is the case, we can write $x = \sum_{i=1}^{M} \sum_{j=1}^{n} \alpha_{ij} v_i \otimes w_j = \hat{x}$, and of course $\hat{x}^T \hat{L} \hat{x} = 0$. Therefore, in order for matrix $\hat{L} + \hat{P}$ to be positive definite, we have to choose matrix P so that $\hat{x}^T (\hat{L} + \hat{P}) \hat{x} > 0$ for every such vector $\hat{x}$.

Note that since

$$\hat{L}\hat{x} = \sum_{i=1}^{N} \sum_{j=1}^{n} \alpha_{ij} \ \lambda_i \mu_j v_i \otimes w_j =$$

$$= \sum_{i=1}^{M} \sum_{j=1}^{n} \alpha_{ij} \ \lambda_i \mu_j v_i \otimes w_j + \sum_{i=M+1}^{N} \sum_{j=1}^{n} \alpha_{ij} \ \lambda_i \mu_j v_i \otimes w_j = 0_{Nn} + 0_{Nn} = 0_{Nn} \tag{A.9}$$

vector $\hat{x}$ can be written as

$$\hat{x} = \begin{bmatrix} \varphi_1 1_{M_1} \otimes z_1 \\ \varphi_2 1_{M_2} \otimes z_2 \\ \vdots \\ \varphi_M 1_{M_M} \otimes z_M \end{bmatrix} \tag{A.10}$$

where $\varphi_i \in \mathbb{R},\ z_i \in \mathbb{R}_n\ \forall i = 1 \ldots M$.

Now let us evaluate

$$\hat{P}\hat{x} = \begin{bmatrix} \varphi_1(P_1 \otimes K)(1_{M_1} \otimes z_1) \\ \varphi_2(P_2 \otimes K)(1_{M_2} \otimes z_2) \\ \vdots \\ \varphi_M(P_M \otimes K)(1_{M_M} \otimes z_M) \end{bmatrix} \tag{A.11}$$

and therefore

$$\hat{x}^T\hat{P}\hat{x} = \begin{bmatrix} \varphi_1(1_{M_1} \otimes z_1)^T & \ldots & \varphi_M(1_{M_M} \otimes z_M)^T \end{bmatrix} \begin{bmatrix} \varphi_1(P_1 \otimes K)(1_{M_1} \otimes z_1) \\ \vdots \\ \varphi_M(P_M \otimes K)(1_{M_M} \otimes z_M) \end{bmatrix} =$$

$$= \varphi_1^2(1_{M_1} \otimes z_1)^T(P_1 \otimes K)(1_{M_1} \otimes z_1) + \ldots + \varphi_M^2(1_{M_M} \otimes z_M)^T(P_M \otimes K)(1_{M_M} \otimes z_M) =$$

$$= \varphi_1^2(p_1\ z_1^T K z_1 + \ldots + p_{M_1}\ z_1^T K z_1) + \ldots + \varphi_M^2(p_{M_{M-1}+1}\ z_M^T K z_M + \ldots + p_{M_M}\ z_M^T K z_M) =$$

$$= \varphi_1^2(z_1^T K z_1) \sum_{i=1}^{M_1} p_i + \ldots + \varphi_M^2(z_M^T K z_M) \sum_{i=M_{M-1}+1}^{M_M} p_i \tag{A.12}$$

Since $\varphi_h^2, z_h^T K z_h > 0\ \forall h \in [1, M]$, from the last expression it is easy to see that in order for $\hat{x}^T\hat{P}\hat{x}$ to be strictly positive we need at least one node in each connected component of the network to be a pin node, meaning that the graph must be pinned. Indeed, in this condition we get

$$\hat{x}^T\hat{P}\hat{x} = 0 + \hat{x}^T\hat{P}\hat{x} = \hat{x}^T\hat{L}\hat{x} + \hat{x}^T\hat{P}\hat{x} = \hat{x}^T(\hat{L}+\hat{P})\hat{x} = \hat{x}^T\tilde{L}\hat{x} > 0 \quad \text{(A.13)}$$

Therefore, since $x^T\hat{L}x > 0\ \forall x \neq \hat{x}$ and as a consequence $x^T\tilde{L}x > 0\ \forall x \neq \hat{x}$, we can say that

$$x^T\tilde{L}x > 0\ \forall x \in \mathbb{R}_{Nn} - \{0_{Nn}\} \quad \text{(A.14)}$$

if and only if each component of the graph contains at least one pin node.

So if we denote with λ the minimum eigenvalue of the augmented Laplacian, we can state that

$$\lambda > 0 \iff \textit{the graph is pinned} \quad \text{(A.15)}$$

□

Bibliography

[1] Reza Olfati-Saber and Jeff S Shamma. Consensus filters for sensor networks and distributed sensor fusion. In *Decision and Control, 2005 and 2005 European Control Conference. CDC-ECC'05. 44th IEEE Conference on*, pages 6698–6703. IEEE, 2005.

[2] Feng Xi, Jin He, and Zhong Liu. Adaptive fast consensus algorithm for distributed sensor fusion. *Signal Processing*, 90(5):1693–1699, 2010.

[3] Reza Olfati-Saber. Flocking for multi-agent dynamic systems: Algorithms and theory. *Automatic Control, IEEE Transactions on*, 51(3):401–420, 2006.

[4] Murat Arcak. Passivity as a design tool for group coordination. *Automatic Control, IEEE Transactions on*, 52(8):1380–1390, 2007.

[5] Dimos V Dimarogonas and Kostas J Kyriakopoulos. A connection between formation infeasibility and velocity alignment in kinematic multi-agent systems. *Automatica*, 44(10):2648–2654, 2008.

[6] Ming Cao, Brian DO Anderson, A Stephen Morse, and Changbin Yu. Control of acyclic formations of mobile autonomous agents. In *Decision and Control, 2008. CDC 2008. 47th IEEE Conference on*, pages 1187–1192. IEEE, 2008.

[7] Florian Dörfler, Michael Chertkov, and Francesco Bullo. Synchronization in complex oscillator networks and smart grids. *Proceedings of the National Academy of Sciences*, 110(6):2005–2010, 2013.

[8] Alex Arenas, Albert Díaz-Guilera, Jurgen Kurths, Yamir Moreno, and Changsong Zhou. Synchronization in complex networks. *Physics Reports*, 469(3):93–153, 2008.

[9] Reza Olfati-Saber and Richard M Murray. Consensus problems in networks of agents with switching topology and time-delays. *Automatic Control, IEEE Transactions on*, 49(9):1520–1533, 2004.

[10] Martin Andreasson, Dimos V Dimarogonas, and Karl H Johansson. Undamped nonlinear consensus using integral lyapunov functions. In *American Control Conference (ACC), 2012*, pages 6644–6649. IEEE, 2012.

[11] Wei Ren and Ella Atkins. Distributed multi-vehicle coordinated control via local information exchange. *International Journal of Robust and Nonlinear Control*, 17(10-11):1002–1033, 2007.

[12] Wei Ren and Randal W Beard. Consensus algorithms for double-integrator dynamics. *Distributed Consensus in Multi-vehicle Cooperative Control: Theory and Applications*, pages 77–104, 2008.

[13] Abdelkader Abdessameud and Abdelhamid Tayebi. On consensus algorithms design for double integrator dynamics. *Automatica*, 2012.

[14] Wei Ren and Randal W Beard. Consensus of information under dynamically changing interaction topologies. In *American Control Conference, 2004. Proceedings of the 2004*, volume 6, pages 4939–4944. IEEE, 2004.

[15] Chai Wah Wu. Agreement and consensus problems in groups of autonomous agents with linear dynamics. In *Circuits and Systems, 2005. ISCAS 2005. IEEE International Symposium on*, pages 292–295. IEEE, 2005.

[16] Reza Olfati-Saber, J Alex Fax, and Richard M Murray. Consensus and cooperation in networked multi-agent systems. *Proceedings of the IEEE*, 95(1):215–233, 2007.

[17] Jinhuan Wang, Daizhan Cheng, and Xiaoming Hu. Consensus of multi-agent linear dynamic systems. *Asian Journal of Control*, 10(2):144–155, 2008.

[18] Jun Zhao, David J Hill, and Tao Liu. Synchronization of complex dynamical networks with switching topology: a switched system point of view. *Automatica*, 45(11):2502–2511, 2009.

[19] Pietro DeLellis, Mario DiBernardo, Franco Garofalo, and Davide Liuzza. Analysis and stability of consensus in networked control systems. *Applied Mathematics and Computation*, 217(3):988–1000, 2010.

[20] Soummya Kar and José Moura. Sensor networks with random links: Topology design for distributed consensus. *Signal Processing, IEEE Transactions on*, 56(7):3315–3326, 2008.

[21] Pietro DeLellis, Mario di Bernardo, Franco Garofalo, and Maurizio Porfiri. Evolution of complex networks via edge snapping. *Circuits and Systems I: Regular Papers, IEEE Transactions on*, 57(8):2132–2143, 2010.

[22] Jun Zhao, David J Hill, and Tao Liu. Synchronization of dynamical networks with nonidentical nodes: Criteria and control. *Circuits and Systems I: Regular Papers, IEEE Transactions on*, 58(3):584–594, 2011.

[23] Guodong Shi and Karl Henrik Johansson. Multi-agent robust consensus-part i: Convergence analysis. In *Decision and Control and European Control Conference (CDC-ECC), 2011 50th IEEE Conference on*, pages 5744–5749. IEEE, 2011.

[24] Lei Wang and Qing-guo Wang. Synchronization in complex networks with switching topology. *Physics Letters A*, 375(34):3070–3074, 2011.

[25] Yao Chen, Wenwu Yu, Fangfei Li, and Shasha Feng. Synchronization of complex networks with impulsive control and disconnected topology. *Proceedings of the 4th IFAC Conference on Analysis and Design of Hybrid Systems*, 2013.

[26] Xiao Fan Wang and Guanrong Chen. Pinning control of scale-free dynamical networks. *Physica A: Statistical Mechanics and its Applications*, 310(3):521–531, 2002.

[27] Xiang Li, Xiaofan Wang, and Guanrong Chen. Pinning a complex dynamical network to its equilibrium. *Circuits and Systems I: Regular Papers, IEEE Transactions on*, 51(10):2074–2087, 2004.

[28] Tianping Chen, Xiwei Liu, and Wenlian Lu. Pinning complex networks by a single controller. *Circuits and Systems I: Regular Papers, IEEE Transactions on*, 54(6):1317–1326, 2007.

[29] Francesco Sorrentino, Mario di Bernardo, Franco Garofalo, and Guanrong Chen. Controllability of complex networks via pinning. *PHYSICAL REVIEW E Phys Rev E*, 75:046103, 2007.

[30] Maurizio Porfiri and Mario di Bernardo. Criteria for global pinning-controllability of complex networks. *Automatica*, 44(12):3100–3106, 2008.

[31] Zhi Hai Rong, Xiang Li, and Wen Lian Lu. Pinning a complex network through the betweenness centrality strategy. In *Circuits and Systems, 2009. ISCAS 2009. IEEE International Symposium on*, pages 1689–1692. IEEE, 2009.

[32] Fuzhong Nian and Xingyuan Wang. Optimal pinning synchronization on directed complex network. *Chaos: An Interdisciplinary Journal of Nonlinear Science*, 21(4):043131–043131, 2011.

[33] Yang-Yu Liu, Jean-Jacques Slotine, and Albert-László Barabási. Controllability of complex networks. *Nature*, 473(7346):167–173, 2011.

[34] Pietro DeLellis, Mario di Bernardo, and Luiz Felipe R Turci. Fully adaptive pinning control of complex networks. In *Circuits and Systems (ISCAS), Proceedings of 2010 IEEE International Symposium on*, pages 685–688. IEEE, 2010.

[35] Pietro DeLellis, Mario di Bernardo, and Maurizio Porfiri. Pinning control of complex networks via edge snapping. *Chaos: An Interdisciplinary Journal of Nonlinear Science*, 21(3):033119–033119, 2011.

[36] Reza Dariani, Arturo Buscarino, Luigi Fortuna, and Mattia Frasca. Effect of motion on pinning control of time-varying networks. In *WIRN*, pages 105–111, 2011.

[37] Jianwen Feng, Shaohui Sun, Chen Xu, Yi Zhao, and Jingyi Wang. The synchronization of general complex dynamical network via pinning control. *Nonlinear Dynamics*, 67(2):1623–1633, 2012.

[38] Qiang Song, Fang Liu, Jinde Cao, and Wenwu Yu. Pinning-controllability analysis of complex networks: An m-matrix approach. *IEEE Transactions on Circuits and Systems. Part 1: Regular Papers*, 59(11):2692–2701, 2012.

[39] Zhou Yan, Xiao-Ling Jin, and Zhi-Long Huang. The local stochastic stability for complex networks under pinning control. *International Journal of Bifurcation and Chaos*, 22(05), 2012.

[40] Massimiliano de Magistris, Mario di Bernardo, Edmondo Di Tucci, and Sabato Manfredi. Synchronization of networks of non-identical chua's circuits: Analysis and experiments. *Circuits and Systems I: Regular Papers, IEEE Transactions on*, 59(5):1029–1041, 2012.

[41] Housheng Su and Xiaofan Wang. Pinning control of complex networked systems. *AMC*, 10:12, 2013.

[42] Paulo Tabuada. Event-triggered real-time scheduling of stabilizing control tasks. *Automatic Control, IEEE Transactions on*, 52(9):1680–1685, 2007.

[43] WPMH Heemels, JH Sandee, and PPJ Van Den Bosch. Analysis of event-driven controllers for linear systems. *International journal of control*, 81(4):571–590, 2008.

[44] Jan Lunze and Daniel Lehmann. A state-feedback approach to event-based control. *Automatica*, 46(1):211–215, 2010.

[45] Daniel Lehmann, Georg Alexander Kiener, and Karl Henrik Johansson. Event-triggered pi control: saturating actuators and anti-windup compensation. In *Decision and Control (CDC), 2012 IEEE 51st Annual Conference on*, pages 6566–6571. IEEE, 2012.

[46] Daniel Lehmann, Jan Lunze, and Karl Henrik Johansson. Comparison between sampled-data control, deadband control and model-based event-triggered control. In *Proceedings of the 4th Conference on Analysis and Design of Hybrid Systems. Eindhoven, Netherlands*, 2012.

[47] Daniel Lehmann, Erik Heriksson, and Karl Henrik Johansson. Event-triggered model predictive control of discrete-time linear systems subject to disturbances. In *European Control Conference*, 2013.

[48] Xiaofeng Wang and Michael D Lemmon. Event-triggered broadcasting across distributed networked control systems. In *American Control Conference, 2008*, pages 3139–3144. IEEE, 2008.

[49] Dimos V Dimarogonas and Karl Henrik Johansson. Event-triggered control for multi-agent systems. In *Decision and Control, 2009 held jointly with the 2009 28th Chinese Control Conference. CDC/CCC 2009. Proceedings of the 48th IEEE Conference on*, pages 7131–7136. IEEE, 2009.

[50] Dimos V Dimarogonas and Karl H Johansson. Event-triggered cooperative control. In *European Control Conference*, pages 3015–3020, 2009.

[51] Maria Guinaldo, Dimos V Dimarogonas, Karl Henrik Johansson, J Sánchez, and Sebastián Dormido. Distributed event-based control for interconnected

linear systems. In *Decision and Control and European Control Conference (CDC-ECC), 2011 50th IEEE Conference on*, pages 2553–2558. IEEE, 2011.

[52] Guodong Shi and Karl Henrik Johansson. Multi-agent robust consensus-part ii: Application to distributed event-triggered coordination. In *Decision and Control and European Control Conference (CDC-ECC), 2011 50th IEEE Conference on*, pages 5738–5743. IEEE, 2011.

[53] Yuan Fan, Gang Feng, Yong Wang, and Cheng Song. Distributed event-triggered control of multi-agent systems with combinational measurements. *Automatica*, 2012.

[54] Georg S Seyboth, Dimos V Dimarogonas, and Karl H Johansson. Event-based broadcasting for multi-agent average consensus. *Automatica*, 2012.

[55] R Aragues, Guodong Shi, Dimos V Dimarogonas, C Sagues, and Karl Henrik Johansson. Distributed algebraic connectivity estimation for adaptive event-triggered consensus. In *American Control Conference (ACC), 2012*, pages 32–37. IEEE, 2012.

[56] Meng Guo and Dimos V Dimarogonas. Nonlinear consensus via continuous, sampled, and aperiodic updates. *International Journal of Control*, 86(4), 2013.

[57] Davide Liuzza, Dimos V Dimarogonas, Mario di Bernardo, and Karl H Johansson. Distributed model based event-triggered control for synchronization of multi-agent systems. In *9th IFAC Symposium on Nonlinear Control Systems*, pages 329–334, 2013.

[58] Adolfo Anta and Paulo Tabuada. To sample or not to sample: Self-triggered control for nonlinear systems. *Automatic Control, IEEE Transactions on*, 55(9):2030–2042, 2010.

[59] Dimos V Dimarogonas, Emilio Frazzoli, and Karl Henrik Johansson. Distributed self-triggered control for multi-agent systems. In *Decision and*

Control (CDC), 2010 49th IEEE Conference on, pages 6716–6721. IEEE, 2010.

[60] WPMH Heemels, Karl Henrik Johansson, and Paulo Tabuada. An introduction to event-triggered and self-triggered control. In *Decision and Control (CDC), 2012 IEEE 51st Annual Conference on*, pages 3270–3285. IEEE, 2012.

[61] Hassan K Khalil. *Nonlinear systems*, volume 3. Prentice hall Upper Saddle River, 2002.

[62] Maurizio Porfiri and Francesca Fiorilli. Node-to-node pinning control of complex networks. *Chaos: An Interdisciplinary Journal of Nonlinear Science*, 19(1):013122–013122, 2009.